Geological Society, London, Special Publications Online First

The long Pleistocene record from the Pego-Oliva marshland (Alicante-Valencia, Spain)

Trinidad Torres, José E. Ortiz, Domingo Martín-Sánchez, Isabel Arribas, Laura Moreno, Bruno Ballesteros, Ana Blázquez, José Antonio Domínguez and Tomás Rodríguez Estrella

Geological Society, London, Special Publications, first published July 22, 2013; doi 10.1144/SP388.2

The long Pleistocene record from the Pego-Oliva marshland (Alicante-Valencia, Spain)

TRINIDAD TORRES[1]*, JOSÉ E. ORTIZ[1], DOMINGO MARTÍN-SÁNCHEZ[1], ISABEL ARRIBAS[1], LAURA MORENO[1], BRUNO BALLESTEROS[2], ANA BLÁZQUEZ[3], JOSÉ ANTONIO DOMÍNGUEZ[2] & TOMÁS RODRÍGUEZ ESTRELLA[4]

[1]*Laboratory of Biomolecular Stratigraphy, E.T.S.I. Minas, Universidad Politécnica de Madrid. C/Ríos Rosas 21, Madrid 28003, Spain*

[2]*Instituto Geológico y Minero e España, C/Cirilo Amorós, 42, 46004 Valencia, Spain*

[3]*Environmental and Marine Sciences Research Institute, Catholic University, Valencia, C/Guillem de Castro 94, 46003 Valencia, Spain*

[4]*Dpto. Ingeniería Minera y Cartografía, Universidad Politécnica de Cartagena, Pso Alfonso XIII 52, 30203 Cartagena, Spain*

**Corresponding author (e-mail: trinidad.torres@upm.es)*

Abstract: Seven borehole cores were analysed to reconstruct the Pleistocene evolution of the Pego-Oliva Basin (Mediterranean coast, Iberian Peninsula). A total of 295 samples were recovered for amino acid racemization (AAR) dating, and 77 samples for sedimentological, palaeontological and biomarker determination, with two objectives: (1) to establish a chronological framework (especially for Middle Pleistocene); and (2) to obtain data on the palaeoenvironment.

(1) AAR proved that the record covers approximately 650 ka in which no important hiatuses occurred, although minor ones cannot be discarded. AAR provided valuable information on differential subsidence rates, and Marine Isotope Stages (MISs) 15–1 were identified.

(2) Litho- and biofacies allowed the identification of distinct palaeoenvironments through time, with the constant presence of a marsh/lagoonal environment with brackish or saline water with continental or marine influence. Remains of marine molluscs allowed the determination of periods of highstand sea level. Biomarkers indicated a constant input from terrestrial plants, and allowed definitions of periods with variable water mass and environmental moisture. As in other Mediterranean littoral areas, facies with a marine influence occurred mainly during odd MISs, indicating periods of highstand sea level. In contrast, alluvial-fan progradation and continental brackish wetlands developed during even MISs.

Coastal wetlands, marshes and salt marshes in the Iberian Peninsula record environmental changes during the Quaternary Period and represent the last evidence of the satellite basins that developed after the Alpine Orogeny period. Given the flat topography of these environments, it is not possible to obtain samples from outcrops, thus it is necessary to use data from boreholes, which in most cases are drilled for other purposes, namely geotechnical and hydrogeological research. In general, coastal wetlands, marshes and salt marshes are characterized by a mixed influence of continental and marine waters, which, when not anoxic, usually have high organic productivity reflected in reducing bottoms with a dominantly fine-grained sedimentation. This favours the preservation of biomarkers, fossil organism shells and organic molecules derived from tissue decay.

These coastal environments are linked to marine–terrestrial transition settings, and thus they share both environmental signals, and can be used to link marine and terrestrial records.

In the Mediterranean realm, coastal plains present favourable characteristics as a result of the microtidal character of the Mediterranean Sea, the lack of hurricane occurrence and the low occurrence of earthquakes (tsunami). Furthermore, coastal deposits are commonly linked to sea-level changes in such a way that periods of lowstand sea level are reflected in stratigraphical gaps, but during active sedimentation periods the record can be considered continuous, although short erosion periods may also occur.

The Mediterranean coast of Spain has been widely studied for the palaeoenvironmental reconstruction of Quaternary times. Until now, such

From: MARTINI, I. P. & WANLESS, H. R. (eds) *Sedimentary Coastal Zones from High to Low Latitudes: Similarities and Differences*. Geological Society, London, Special Publications, **388**, http://dx.doi.org/10.1144/SP388.2

studies have focused mainly on marine raised deposits, whose elevations, faunal remains, radiometric age (Goy *et al.* 1986; Hillaire-Marcel *et al.* 1986; Causse *et al.* 1993; Fumanal *et al.* 1993*a*; Viñals 1995*a*, *b*; Zazo 1999; Zazo *et al.* 2003) and amino acid chronology (Hearty 1986, 1987; Hearty *et al.* 1986; Torres *et al.* 2000, 2010; Ortiz *et al.* 2004*c*) indicated highstand sea levels linked to interglacial stages. However, these deposits are discontinuous. Information about present-day offshore deposits has been provided by Fumanal *et al.* (1993*a*), Rey & Fumanal (1996*a*), Dupré *et al.* (1988) and Blázquez (2005).

The pollen content of some continental sequences in coastal areas (Pérez-Obiol & Julia 1984; Fumanal & Dupré 1986; Burjachs & Juliá 1994; Yll *et al.* 1994; Badal & Roiron 1995; Carrión & Dupré 1996; Carrión & van Geel 1999; Carrión *et al.* 1999) and caves has also been used for late Pleistocene–Holocene palaeoclimatic reconstruction (Carrión 1992; Carrión *et al.* 1995; Carrión & Munuera 1997). Likewise, the following marshes have been examined in the Spanish Mediterranean realm (Fig. 1): Peñíscola (Usera *et al.* 2006), Torreblanca (Collado & Robles 1983; Segura *et al.* 1997), Jávea (Fumanal *et al.* 1993*b*; Usera *et al.* 2002), Gandía and La Safor (Viñals 1995*a*), Moraira (Viñals 1995*b*), and Albufereta in Alicante (Blázquez & Ferrer 2003; Ferrer *et al.* 2005), but all of these have short sequences that only cover the Holocene. Extensive coastal records are scarce, and it was only in the Elche Basin (Fig. 1a) that numerous boreholes were drilled and studied in detail (Blázquez 2005; Blázquez & Usera 2010). These cores are up to 30 m long, but several gaps are present and, thus, they do not provide a continuous record. Their microfossil content, together with sedimentological and magnetic susceptibility, enabled a reconstruction to be made of the palaeoenvironmental evolution of the Elche lagoon area (SE Spain) during the Quaternary. Previous studies have addressed the Upper Pleistocene record of the Pego-Oliva wetland: Dupré *et al*. (1988), Mateu (1989), Viñals *et al.* (1989), Hernández Ruiz *et al.* (1993), Viñals & Fumanal (1995), Viñals (1996) and Mateu *et al.* (1997) obtained their results from six borehole cores and 90 stratigraphical profiles that show the uppermost 50 m of the record. However, some age discrepancies were observed in various thermoluminiscence ages (Viñals & Fumanal 1995; Viñals 1996), as MIS 5 was placed at a depth of 50 m in some parts of the Pego-Oliva Basin, whereas in other areas it was located at a depth of about 20 m. Durán *et al.* (2005) reconstructed a simple palaeogeography with alluvial-fan sediments landwards, grading into fine-grained marsh deposits that interfinger seawards with aeolian sands. In Dupré *et al.* (1988), Viñals *et al.* (1989), Viñals (1996) and the present paper, these sands are interpreted to be of marine origin. Ballesteros Navarro *et al.* (2009) drilled seven borehole cores for hydrogeological purposes.

Therefore, the lack of continuity of the records seriously restricts our understanding of the palaeoenvironmental evolution of the Iberian coast, and the western Mediterranean Sea in general. Only in the lower part of the Guadalquivir Basin, along the Atlantic Ocean, was the sedimentary evolution of the Guadalquivir marshlands (Fig. 1a) during the Upper Pliocene and Pleistocene reconstructed (Salvany *et al.* 2011). In this regard, the Pego-Oliva marshland (Fig. 1), with more than 140 m cored in its deepest zone, with abundant fossil and plant remains, is a suitable area for the interpretation of prolonged palaeoenvironmental conditions in the Spanish Mediterranean realm. Records of this nature are uncommon in this area as deposits of these ages generally consist of discontinuous raised marine deposits.

Thus, the main aims of this study were as follows: (1) to establish the complete chronological framework (especially the Middle Pleistocene) of the Pego-Oliva marshland (through amino acid racemization (AAR)); (2) to test the presence/absence of long hiatuses; (3) to determine the palaeoenvironmental conditions of the marshland through the fossil content, especially for the Middle Pleistocene; and (4) to obtain insights into the plant cover of the marsh and surrounding areas from the biomarkers preserved in the sediments, especially for the Middle Pleistocene time span.

Geographical and geological setting

The Pego-Oliva Basin extends over 12.9 km^2 near the village of Pego in the provinces of Alicante and Valencia (eastern Spain) (Fig. 1). In the last few centuries, the extension of the Pego-Oliva marsh has diminished as result of agricultural practices. A sand barrier capped with small dunes separates the marsh from the Mediterranean Sea (Figs 1 & 2d).

The zone is extensively cultivated on the alluvial-fan slopes, in which terraced fields allowed (since Moorish times) the cultivation of olive, cherry and almond trees. Today, orange trees and orchard products comprise the main agricultural production, and, on the marsh border, there are many rice crops, which are generally in conflict with the conservation policy for the marshland area.

The Pego-Oliva area has been subjected to vigorous land reclamation over the last century, although today it is a protected area (Natural Park). Owing to agricultural practices, the multilayered aquifer has been under observation for

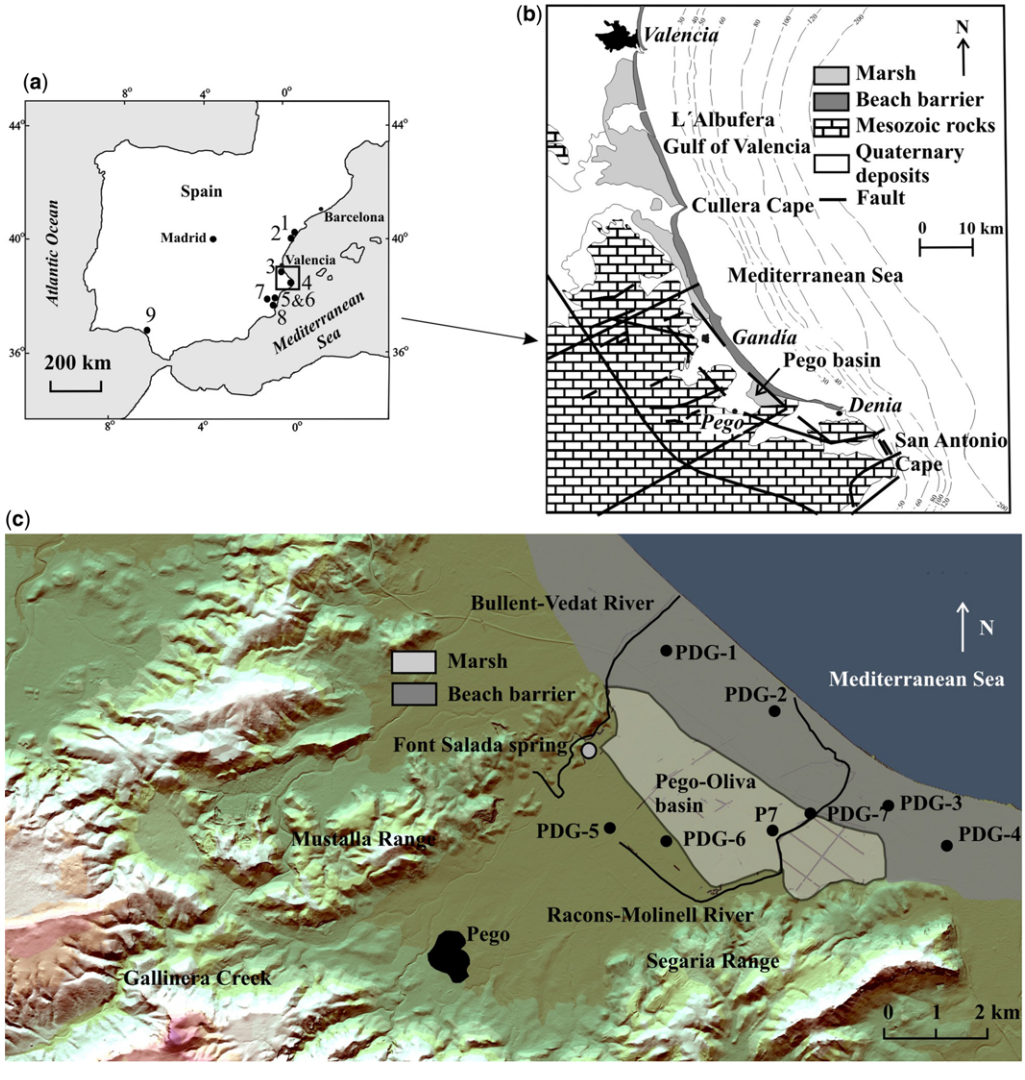

Fig. 1. Geographical location of the Pego-Oliva Basin. (**a**) General location in eastern Spain together with other marshlands. (**b**) Generalized geological map of the Pego-Oliva Basin (modified from Rey & Fumanal 1996*a*). (**c**) Location of boreholes drilled, including P7 of Dupré *et al.* (1988). (1, Peñíscola; 2, Torreblanca; 3, Albufera; 4, Jávea, Gandía, La Safor and Moraira; 5, Albufereta of Alicante; 6, Santa Pola; 7, Elche; 8, Mar Menor; 9, Guadalquivir marshlands).

many decades. During the last century, a number of boreholes were drilled and geophysics (electrical resistivity) campaigns were undertaken (Hernández Ruiz *et al.* 1993). The results of this work were completed in Viñals (1996). As marine water intrusion became considerable as a result of intense groundwater extraction, the Spanish Geological Survey drilled seven boreholes to monitor water quality, which was seriously threatened by this intrusion.

The basin developed between two craggy sierras, Mustalla to the north and Segaria to the south, both comprising Upper Cretaceous calcareous rocks (Senonian) affected by Alpine tectonics. These rocks are deeply karstified with a complex relationship between the underground karst waters and the marsh hydrogeology. Near the northern boundary of the marsh, there is an active saline spring (Font Salada, Fig. 2a, b) that has fed the marsh in the past. Isotope geochemistry (Ballesteros Navarro

Fig. 2. Representative photographs of the Pego-Oliva Basin. (**a**) & (**b**) Drainage channel and pond, respectively, of the Font Salada spring. (**c**) General view of the Pego-Oliva marshland basin. (**d**) Beach and coastal dunes.

et al. 2006, 2009) indicates that the spring water is of marine origin. Marsh deposits lie on impervious sediments (marls) of Miocene age. Two small but perennial rivers (Bullent-Vedat and Racons-Molinell), both karst-water related, feed the marsh. The Racons-Molinell River is connected to the Mustalla creek and has its catchment in the west of the study area (Fig. 1c), being the origin of the main alluvial fan responsible for the catastrophic floods that have affected the Pego village in the past and which are recorded in the geological record (Viñals & Fumanal 1995; Viñals 1996).

As a result of Alpine tectonics during the Miocene, a series of roughly east–west-orientated satellite basins opened towards the Mediterranean, and were filled with a series (partially exposed) of Miocene–Pliocene and Pleistocene deposits (Champetier 1972; Goy & Zazo 1974; Dumas 1977; Rodríguez Estrella 1977; Pulido 1979) (Fig. 1). Some of these basins still remain active as barred lagoons (e.g. Mar Menor, Albufera de Valencia: Fig. 1a) and marshlands (e.g. Pego-Oliva). Almost all of them are severely affected by reclamation after intensive drainage. In other cases, the lagoonal and marsh deposits are overlain by saline (solonchak) and red (terra rossa) soils and caliches.

Although the current geomorphological framework of the Pego-Oliva Basin seems to be simple (alluvial fans, saline springs and marine water intrusions), it does not reflect the geomorphology that controlled the sedimentation during Pleistocene times. This is a tectonic basin in which subsidence favours sedimentary processes from both continental and marine environments; however, it is also affected by erosive processes (Viñals 1996; Ballesteros *et al.* 2009). The development of the Pego-Oliva marsh is directly related to groundwaters. From marine seismic profiles, Díaz del Río *et al.* (1986), Rey & Fumanal (1996*b*) and Viñals (1996) identified bars and beach-rock that controlled the marsh and lagoonal environment during the Late Pleistocene, the shoreline being more than 7 km seawards in some periods. Likewise, local subsidence processes occurred and the basin-basement geometry was initially interpreted using geophysics by Viñals (1996). Ballesteros Navarro *et al.* (2009) reinterpreted the basin geology, providing geophysical data that showed the presence of a complex

system of normal fault-limited blocks (Fig. 3). Some of these still-active blocks are responsible for a number of very recent earthquakes (Rueda & Mézcua 2002). These observations imply that the geomorphology of the basin during the Middle Pleistocene differed considerably from that of the Holocene.

At present, the basin receives water from Bullent-Vedat and Racons-Molinell rivers, but also has a close relationship with groundwater systems (Ballesteros *et al.* 2009); that is, it receives discharges from lateral karstic aquifers and from a basal detrital aquifer, although anthropogenic factors also affect hydrodynamics in the Pego-Oliva marshland. The Font Salada saline spring water presents a very high chlorine (NaCl) concentration, ranging between 800 and 1020 $\mu g\,l^{-1}$, SO_4^{2-} being very stable around 100 $\mu\,l^{-1}$, and a water temperature that varies between 18 and 20 °C (Ballesteros Navarro *et al.* 2008). In the spring zone, a peculiar biota developed, including algae and upper plants that also appear in the marsh zone: Cyanophyceae (13 species), Rhodophyceae (six species), Clorophyceae (nine species), Ulvophyceae (eight species), Charophyceae (18 species), Xantophyceae (two species) and Bacillariophyceae (four species) have been described (Cantoral & Aboal 2001; Egidos & Aboal 2003). From the 51 diatomea taxa identified (Cantoral & Aboal 2008), 25 correspond to brackish-water environments, seven to freshwater and 35 are cosmopolites, being noteworthy that five species show tropical affinities. In the marsh, *Phragmites australis* and *Tamaryx gallica* are the dominant upper plants. However, in the sierras (where wildfires did not affect the biome), *Pinus* sp., *Taxus baccata* and *Quercus* sp. dominate, and near the creek bottoms *Populus* sp, *Fraxinus* sp., *Salix* sp. and other caducifolia are common.

Study design, materials and methods

In recent years, a series of seven boreholes (Table 1, Figs 1c & 4) with continuous core recovery were drilled inside the marsh dominion for hydrogeological control purposes (Ballesteros Navarro *et al.* 2009). The cores were stored in the sample archive of the Geological Survey of Spain (IGME), located in Peñarroya (Córdoba). In 2010, we sampled these boreholes to study their sedimentological characteristics, fossil content and organic compounds to ascertain the Pleistocene palaeoenvironmental evolution of the Pego-Oliva marsh. The cores were also sampled for amino acid racemization (AAR) dating in order to place all of the palaeoclimatological variations into a chronological framework.

We established the core lithology using descriptions given in an internal report of the IGME (Ballesteros Navarro *et al.* 2008), although some minor simplifications were also made (Fig. 4). Borehole PDG5 reached the Miocene basement at a depth of 52.2 m, whereas PDG6 reached the Upper

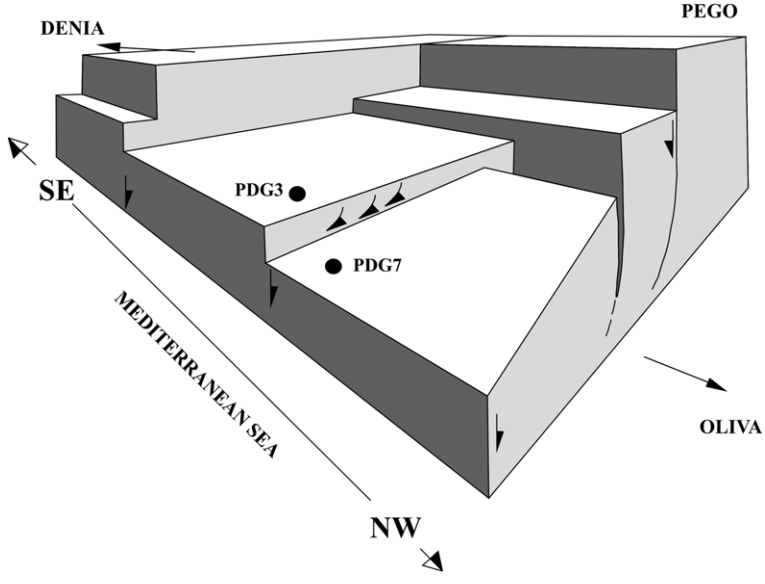

Fig. 3. Basement structure based on geophysics, with the position of PDG7 and PDG3 boreholes shown (modified from Viñals 1996).

Table 1. *Coordinates (UTM) of the boreholes used for this study*

Borehole	Latitude (°)	Longitude (°)	Elevation (m a.s.l.)
PDG1	754.672	4.309.389	1.36
PDG2	756.812	4.308.319	1.38
PDG3	758.966	4.306.480	2.06
PDG4	757.414	4.306.352	3.66
PDG5	753.552	4.306.034	3.45
PDG6	754.575	4.305.837	0.74
PDG7	757.414	4.306.352	1.05

m a.s.l., metres above sea level.

Cretaceous karstified limestones at 78 m. The other cores did not reach the basement, although core PDG7 perforated 140 m of the Pleistocene deposits.

In order to monitor the Pego-Oliva multilayer aquifer, the borehole distribution was roughly T-shaped (Fig. 1c): PDG1, PDG2, PDG3 and PDG4 were drilled directly on the present-day barrier at approximately 250–400 m from the shoreline, and PDG1 and PDG4 were at the seawards foot of the Sierra Mustalla and the Sierra Segaria, respectively. PDG7 was drilled in the SE corner of the Pego-Oliva marsh, and PDG5 and PDG6 were placed in the inner part of the basin, in a zone formerly included in the past extension of the marshland but which is now dry.

We focused the palaeoenvironmental interpretation on the cores from boreholes PDG7 and PDG2 because they were the deepest ones, and held fine-grained deposists that gave large amounts of macro- and microfossil remains. The deposits of the other cores were not dated because there was a dominance of coarse-grained gravels, and their age was considered uncertain. Nevertheless, some horizons of borehole PDG3 were dated for correlation purposes.

We refer to the borehole horizons by their depth, in metres, from top to bottom (sample PDG7-115.40 is at 115.40 m in borehole PDG7). Of note, during drilling operations the sand layers were poorly recovered, thus causing some uncertainties about their true thickness.

AAR dating

The AAR method is based on the premise that almost all living material contains only L-amino acids, which gradually turn into D-amino acids after death in a process known as racemization (Hare 1969). After death, the D/L ratio increases over time until it reaches a value of 1, when a dynamic equilibrium is reached. Thus, racemization ratios can be used to obtain bed correlation because

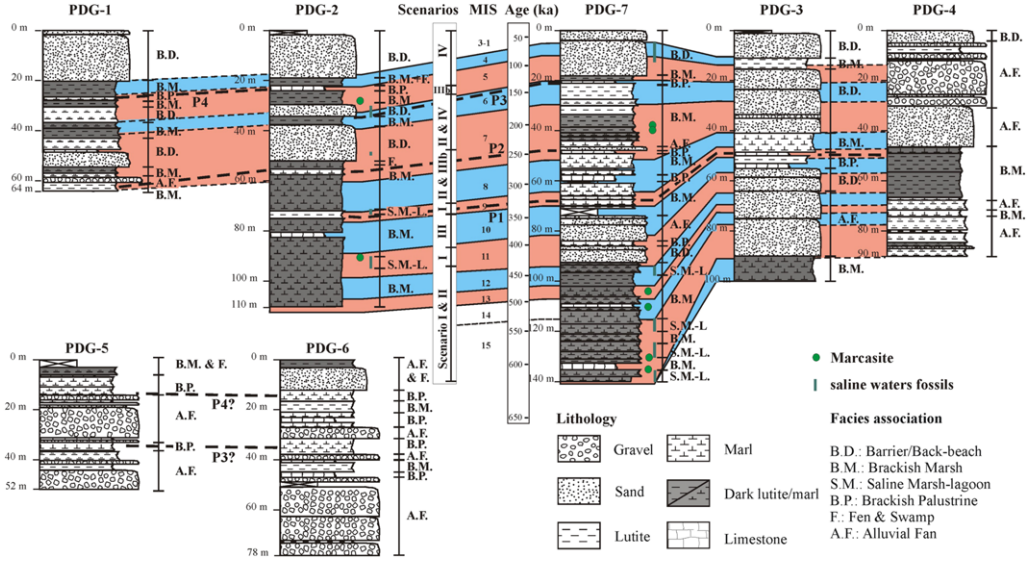

Fig. 4. Fence diagram correlating the borehole sections based on the AAR datings. The correlation was performed based on MIS episodes, although MIS 4–MIS 1 were not separated because the uppermost sand beds were mixed due to drilling operations. Dashed lines mark the tentative correlation between boreholes that are not dated. Dark dashed lines mark the correlation of palustrine carbonate horizons (P). The environmental interpretation of the sedimentary facies associations are also indicated in each borehole.

similar D/L values indicate isochrony. However, the AAR method is not a numerical dating technique in isolation but requires calibration with previously dated samples (through radiometric dating methods) in order to obtain age calculation equations. This process is both genus- and temperature-dependent, so these algorithms can be calculated only from samples located in areas with the same thermal history.

To establish the chronology of the Pego-Oliva marsh record, we sampled cores from boreholes PDG2, PDG3 and PDG7 for AAR dating: 84 samples from 19 horizons of PDG2, 35 from six horizons of PDG3 and 176 samples from 28 horizons of PDG7 (Tables 2–4). Ostracode valves from various species were recovered, although we selected only *Cyprideis torosa* (Jones) individuals for the analysis because it was the only species present in all horizons.

Ostracode valves were carefully cleaned sonically in distilled deionized water and rinsed in the same water to remove sediment. In order to remove secondary organic molecules adsorbed to the shells, the valves were then submerged in 3% hydrogen peroxide for 2 h following Kaufman (2000) and Hearty *et al.* (2004). Only translucent specimens were selected for the analysis, and a single valve of *Cyprideis torosa* specimens was used for each analytical sample. When possible, we performed seven analyses of the same bed. The number of samples from each bed is shown in Tables 2–4. Amino acid concentrations and ratios were quantified using high-performance liquid chromatography (HPLC) in the Biomolecular Stratigraphy Laboratory, following the sample preparation protocol described by Kaufman & Manley (1998) and Kaufman (2000). This procedure involves hydrolysis, which was performed under N_2 atmosphere in 7 μl of 6 M HCl for 20 h at 100 °C. The hydrolysates were evaporated to dryness in *vacuo*, and then rehydrated in 7 μl of 0.01 M HCl with 1.5 mM sodium azide and 0.03 mM L-*homo*-arginine (internal standard). Samples were injected into an Agilent-1100 HPLC equipped with a fluorescence detector. Excitation and emission wavelengths were programmed at 335 and 445 nm, respectively. A Hypersil BDS C18 reverse-phase column (5 μm; 250 × 4 mm i.d.) was used for the analysis.

Aspartic acid and glutamic acid D/L values were selected for the age calculation because in most ostracode valves they account for in excess of about 50% of the amino acid content (Kaufman 2000; Bright & Kaufman 2011). The numerical age of each bed was determined by introducing the aspartic acid and glutamic acid D/L values obtained in *C. torosa* valves collected at each level into the age calculation algorithms established by Ortiz *et al.* (2004*b*). The age of a single bed is the average of the numerical dates obtained for each amino acid D/L value measured in ostracodes from that level, and the age uncertainty is the standard deviation of the numerical ages calculated in each level.

Amino acid racemization is a time- and temperature-controlled chemical reaction. However, the use of the age calculation algorithms obtained in central and southern Spain ostracodes by Ortiz

Table 2. *Mean values and standard deviation of D/L ratios of aspartic acid and glutamic acid obtained in Cyprideis torosa ostracode from the PDG2 borehole core, and age calculation of each level*

Level	*N*	D/L Asp	D/L Glu	Age (ka BP)
5	2	0.151 ± 0.001	0.048 ± 0.001	6.1 ± 0.3
6	1	0.159	0.041	5.1 ± 3.3
17	2	0.238 ± 0.019	0.061 ± 0.018	34.4 ± 7.7
26.5	7	0.351 ± 0.021	0.111 ± 0.015	111.9 ± 20.9
32.3	3	0.352 ± 0.006	0.127 ± 0.012	119.3 ± 10.5
34.5	3	0.413 ± 0.027	0.152 ± 0.010	167.2 ± 24.8
34.9	7	0.414 ± 0.023	0.157 ± 0.026	180.7 ± 25.6
52.6	5	0.460 ± 0.039	0.174 ± 0.030	236.7 ± 42.6
58.5	7	0.473 ± 0.035	0.188 ± 0.040	231.0 ± 57.8
61.1	7	0.516 ± 0.026	0.204 ± 0.017	276.8 ± 56.1
71.3	4	0.507 ± 0.018	0.227 ± 0.033	292.4 ± 32.6
88.6	6	0.531 ± 0.028	0.259 ± 0.033	346.3 ± 45.5
91	3	0.601 ± 0.010	0.360 ± 0.025	464.9 ± 48.0
99.5	5	0.520 ± 0.030	0.285 ± 0.026	352.0 ± 41.9
101.7	4	0.591 ± 0.015	0.344 ± 0.042	442.1 ± 59.4
104.6	7	0.610 ± 0.016	0.368 ± 0.030	483.2 ± 58.9
110.0	7	0.626 ± 0.020	0.412 ± 0.038	538.3 ± 63.0

Table 3. *Mean values and standard deviation of D/L ratios of aspartic acid and glutamic acid obtained in Cyprideis torosa ostracode from the PDG3 borehole core, and age calculation of each level*

Level	*N*	D/L Asp	D/L Glu	Age (ka BP)
9	7	0.206 ± 0.018	0.058 ± 0.003	35.5 ± 4.0
11	1	0.275	0.078	47.9 ± 14.6
21.2	9	0.377 ± 0.022	0.123 ± 0.014	136.5 ± 28.5
41.8	4	0.468 ± 0.008	0.238 ± 0.027	251.9 ± 21.8
51.8	7	0.592 ± 0.023	0.338 ± 0.045	447.4 ± 70.0
72.8	7	0.607 ± 0.028	0.343 ± 0.032	518.5 ± 72.7

et al. (2004*b*) for the dating of the Pego-Oliva record is justified because a similar thermal history (current mean annual temperature of *c.* 15 °C) can be inferred for these areas and the Pego-Oliva Basin, which are all located in the Mediterranean climatic zone of the Iberian Peninsula.

The Asp and Glu D/L values obtained in the ostracode valves are comparable to those found in other laboratories using the same or other techniques. Three samples from an interlaboratory AAR exercise (Wehmiller 1984) analysed by 11 laboratories were used for the comparison of results: ILC-A (*Saxidomus* sp. *c.* 50 ka), ILC-B (*Mercenaria* sp. between 100 and 250 ka) and ILC-C (*Mercenaria* sp. *c.* 1 Ma). The lack of bias and the validity of the process fit provided by our laboratory were confirmed (Table 5). The results from a recent interlaboratory comparison exercise showed that instrumental differences are even smaller than those encountered in the original 1984 study (Wehmiller *et al.* 2010).

Biomarker analysis

A total of 46 samples from the PDG7 core and 31 samples from the PDG2 core were collected for biomarker analysis. Between 4.4 and 9.2 g of

Table 4. *Mean values and standard deviation of D/L ratios of aspartic acid and glutamic acid obtained in Cyprideis torosa ostracode from the PDG7 borehole core, and age calculation of each level*

Level	*N*	D/L Asp	D/L Glu	Age (ka BP)
1.4	1	0.176	0.040	0.9 ± 1.1
6	4	0.272 ± 0.035	0.077 ± 0.011	46.4 ± 21.4
12	7	0.250 ± 0.040	0.070 ± 0.009	33.2 ± 10.8
25.5	7	0.430 ± 0.025	0.167 ± 0.028	182.7 ± 28.6
26.2	7	0.448 ± 0.036	0.189 ± 0.045	193.0 ± 37.6
27.8	7	0.434 ± 0.026	0.148 ± 0.021	173.1 ± 40.1
34.9	7	0.498 ± 0.015	0.185 ± 0.021	242.1 ± 56.2
43.25	7	0.503 ± 0.035	0.198 ± 0.043	256.8 ± 72.2
50.0	7	0.504 ± 0.048	0.277 ± 0.073	298.2 ± 79.2
59.5	7	0.535 ± 0.014	0.245 ± 0.029	320.4 ± 46.3
84.2	7	0.572 ± 0.043	0.276 ± 0.038	383.2 ± 99.2
87.6	7	0.554 ± 0.038	0.268 ± 0.058	383.9 ± 78.7
95	6	0.538 ± 0.005	0.259 ± 0.035	325.9 ± 49.7
97.3	7	0.581 ± 0.033	0.303 ± 0.053	403.8 ± 91.3
102.4	7	0.648 ± 0.017	0.427 ± 0.048	579.4 ± 89.4
109.6	7	0.619 ± 0.015	0.369 ± 0.030	511.7 ± 54.6
111.2	7	0.580 ± 0.022	0.281 ± 0.032	464.0 ± 71.8
115.4	7	0.620 ± 0.051	0.384 ± 0.090	561.6 ± 78.3
120.2	3	0.657 ± 0.017	0.442 ± 0.059	606.9 ± 88.7
126.2	5	0.678 ± 0.012	0.463 ± 0.042	659.9 ± 94.9
127	3	0.638 ± 0.068	0.408 ± 0.103	560.8 ± 163.7
130.8	7	0.636 ± 0.031	0.403 ± 0.069	575.7 ± 103.8
131.2	7	0.644 ± 0.021	0.400 ± 0.014	575.6 ± 81.4
136	7	0.625 ± 0.033	0.485 ± 0.060	597.0 ± 96.8
137.8	7	0.684 ± 0.040	0.535 ± 0.065	740.8 ± 140.3

Table 5. *Asp and Glu D/L values measured in interlaboratory comparison (ILC) samples in the interlaboratory results (ILR) exercise (Wehmiller 1984) and in the Biomolecular Stratigraphy Laboratory of Madrid (LEB)*

Amino acid	Laboratory	ILC-A	ILC-B	ILC-C
Asp D/L	LEB	0.401 ± 0.006	0.719 ± 0.010	0.884 ± 0.015
	ILR	0.378 ± 0.056	0.705 ± 0.056	0.894 ± 0.158
Glu D/L	LEB	0.225 ± 0.003	0.464 ± 0.004	0.902 ± 0.010
	ILR	0.203 ± 0.022	0.432 ± 0.034	0.849 ± 0.070

sediment per sample were dried at 50 °C for 24 h and then ground. Biomarkers were extracted in an accelerated solvent extractor (Dionex ASE 200) using dichloromethane–methanol 2:1 at 1500 psi and 175 °C. The heating phase was 8 min and the static extraction time was 5 min.

The isolated lipid extract was concentrated to dryness using a rotary evaporator, and redissolved in 1 ml of dichloromethane at the time of analysis by gas chromatography (HP 6890) with mass selective detector (HP 5973) and an ATM-5 column (250 × 0.25 mm; 0.20 μm), using helium as the carrier gas.

Results

Chronology

The D/L ratios of aspartic acid and glutamic acid measured in the 295 analytical samples from the cores of PDG2, PDG3 and PDG7 are shown in Tables 2–4, together with the age of each horizon.

The sedimentation rate for each core was calculated by plotting the age of each bed against its depth in metres (Fig. 5). The slopes of the AAR ages v. depth represent the sedimentation rate. High correlation coefficients were observed in the three cores, and were similar for PDG2 and PDG7 (Fig. 5). In PDG3, the slope of the regression line was markedly steeper, indicating that the sedimentation rate was lower in this area. Thus, the amino acid chronology revealed that the stratigraphic record covered a time span of approximately 650 ka (Fig. 4). A good correlation was detected between the chronological framework for the Pego-Oliva Basin obtained through AAR and the thermoluminescence ages of 72 ± 11 and 68 ± 10 ka reported by Dupré *et al.* (1988) obtained at depths of 14.0 and 15.0 m, respectively. These ages were obtained in the core of borehole P7, which was drilled close to PDG7 and PDG2 (Fig. 4). Furthermore, Viñals & Fumanal (1995) used thermoluminescence to date a sand bed at a depth of about 20 m in P7 at 119 ± 18 ka. In this regard, Viñals (1996) provided ages of 58 ± 9 and 107 ± 16 ka in borehole P6 at depths of 10 and 15 m, respectively, and dated beds at a depth of 15 and 19 m at 55 ± 8 and 105 ± 16 ka, respectively, in borehole P9. The ages determined by this method are consistent with those we found using AAR. In contrast, Viñals & Fumanal (1995) dated a sand bed at a depth of 45 m in P1 at 112 ± 17 ka through thermoluminescence. This age seems to be inaccurate as it does not correspond

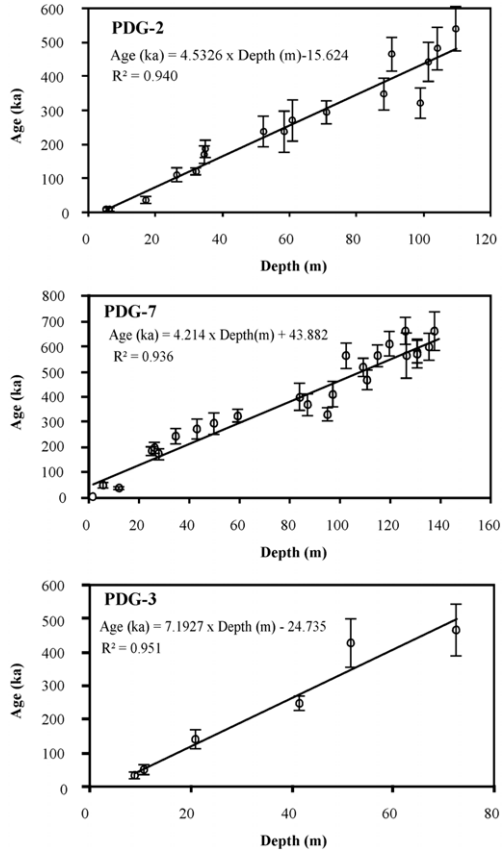

Fig. 5. Correlation diagrams between AAR age (ka) v. depth (m) for the PDG2, PDG3 and PDG7 cores.

either with our dates or with those of Dupré *et al.* (1988), Viñals & Fumanal (1995) or Viñals (1996).

Lithology

We grouped the lithologies into five groups.

(1) Peaty deposits (F) are characterized by the dominance of plant debris over terrigenous sediments and are common in the Holocene Pego-Oliva record but scarce in Pleistocene beds. They are 20 cm thick and appear to have developed in spots, with the exception of the shallower (Holocene) deposits of PDG5 and PDG6. There are two peaty beds in PDG2 at a depth of 53.3 and 20.0 m. Viñals (1996) described peaty beds in four boreholes (different to those used in this study) at a range of depths (lower than 20 m), and in subaereal deposits. These deposits contained subangular medium-sized quartz grains and deeply abraded foraminifera tests.

(2) Massive lutites (Fm) are well represented in all the cores, with the exception of PDG5 and PDG6. They show high carbonate content (>50% according to Viñals 1996). Clay particle size dominates over silt size, and there are disseminated quartz grains. Very abundant mica flakes and minor other minerals occur. On the basis of their colour, it is possible to distinguish two kinds of lutite: grey-black (Fmb) and yellow-brown (Fmy).

Fmb: in addition to its colour, which varies from light grey to black, the most distinctive characteristic of these lutites is the presence of marcasite (Fig. 6f), which appears isolated, forming spheruli and framboids or casting of plant debris or carpeting shells with cockscomb microcrystal clusters. Upper plant remains (indet. seeds and cuticuli) also appear.

Fmy: there is a clear lack of iron sulphides but brown-red patches suggest that, in some cases, marcasite formed, later being oxidized. Carbonation, although not dominant, developed and carbonate root casts appear. Sparse pedogenetic calcium-carbonate noduli also occur.

(3) Marls and limestones (M), which are yellow or white. They contain scarce quartz grains and abundant brackish-water fossils.

(4) Sands (S). Along the borehole records, a series of sand interbeds were identified. Although the core recovery is very poor, these beds are loosely carbonate cemented. Two types of sands can be identified on the basis of the presence/absence of bioclasts, namely siliciclastic (Sa) and bioclastic (Sb) sands.

In the lower and central part of the records, they appear (Sa) as homometric fine-grained quartz sands with very scarce bioclasts, mica flakes and resistant heavy minerals. They constitute the typical detrital layers of the aquifers of the zone and are karstified when carbonate cemented.

At the top of all the borehole records, with the exception of PDG5 and PDG6 in which peaty deposits are common, thick sand beds are observed (Sb) up to 20 m thick. In the core boxes, they appear as a black slurry, and, under the microscope, as fine-grained quartz sand (quartz 80%, limestone 20%). The quartz grains show low roundness, although some attested eolinization and have a high sphericity. Mica flakes are frequent. Bioclasts are very abundant: planktonic and bentonic forams, pelecypoda, gastropods, *Dentalium*, sea urchin spicles, briozoans and unidentifiable fragments. In some cases, bioclasts are black tanned (organic matter). The organic-rich 'black fine-grained' matrix stains the slurried core black.

(5) Gravels (G). Although gravel beds were estimated as thick deposits in the upper part of cores PDG5 and PDG4, and at the bottom of PDG6, they are poorly known because the poor core recovery during the drilling operations did not allow some coarse clasts and possible finer-grained material from interbeds to be retrieved. The scarce gravels are well rounded and made up of Cretaceous limestone clasts.

Fossil content

A large number of ostracode valves were recovered from almost all of the samples in the PDG7 and PDG2 cores (only six samples were barren from a total of 84), the presence of *C. torosa* (Fig. 6d) being continuous along the entire length of the boreholes. In general, the valves were well preserved, being translucent in most cases. However, black-stained valves were also present in some cases; articulated valves in life position were also common. Other ostracode genera, including *Semicytherura*, *Cytherella*, *Loxoconcha* (Fig. 6g), *Cytheroptheron*, *Cushmanidea*, *Cytherois*, *Carinocythereis*, *Hemicyprideis* and *Aurila,* were recovered together with *C. torosa* in some samples. These genera are common inhabitants of the intertidal and circalittoral zones in marine coastal areas of temperate zones (Guillaume *et al.* 1985), although *Loxoconcha*, *Cyprideis* and the non-marine ostracode *Eucypris* can also be found in highly saline marshes, lagoons and continental ponds, such as: Salines Lake, eastern Spain (Roca & Julià 1997); Sebkha Melalla, Algeria; Hassi el Mejna, Daiet el

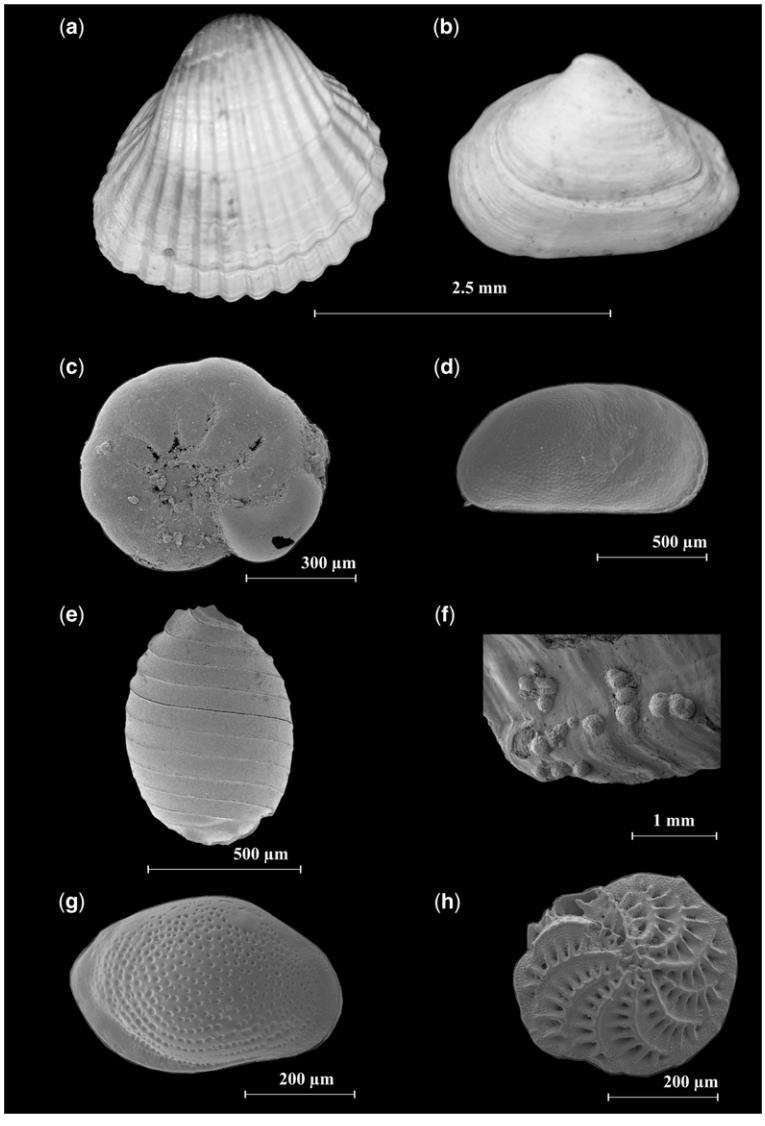

Fig. 6. Pictures of fossil remains from the Pego-Oliva record. (**a**) *Cerastoderma glaucum*. (**b**) *Scrobicularia plana*. (**c**) *Ammonia beccarii*. (**d**) *Cyprideis torosa*. (**e**) *Chara* sp. (**f**) *C. glaucum* shell with marcasite framboids. (**g**) *Loxoconcha elliptica*. (**h**) *Elphidium crispum*.

Melah and Hassi Cheikh, northern Sahara (Fontes *et al.* 1985; Gasse *et al.* 1987); Lake of Tunis, Tunisia (Carbonel & Pujos 1982); and the Guadix-Baza Basin, southern Spain (Ortiz 2000). Notwithstanding, the samples containing these genera were considered to be deposited under brackish–saline conditions. Only in two samples were *Herpetocypris reptans* individuals – typical of water bodies with a low salinity (De Deckker 1981) – found together with *C. torosa* representatives (marked with a black dot in Fig. 7).

Foraminifera tests were present in most samples of PDG7, with the exception of nine horizons (10.0, 19.0, 38.65, 66.0, 95.0, 95.6, 115.30 and 139.40). We separated the foraminifera species into two assemblages: autochthonous and allochthonous associations. Allochthonous foraminifera indicates resedimented tests (from contemporary environments) and reworked tests coming from older strata, while the autochthonous association consists of indigenous specimens. The autochtonous association consisted of *Miliolinella eburnea*

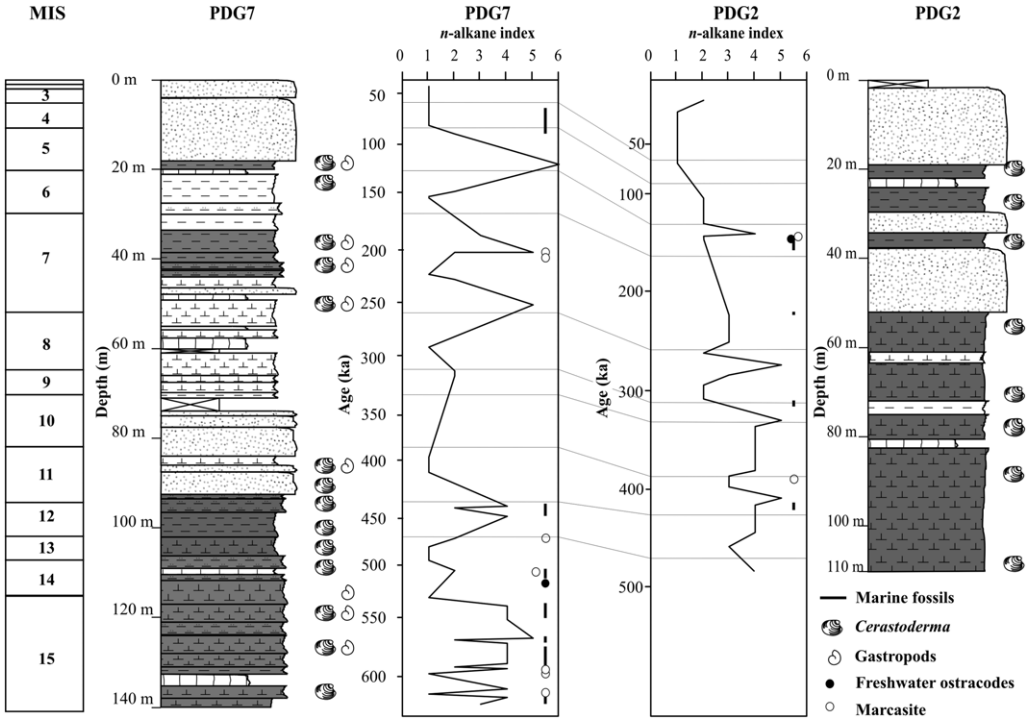

Fig. 7. Downcore plots in PDG7 and PDG2 of the lithologies and the *n*-alkane groups. Chronology and MIS episodes are also shown. Chronology was based on the correlation equations of Figure 5.

(D'Orbigny), *Ammonia becarii tepida* (Lin.) (Fig. 6c), *Elphidium excavatum* (Terquem) (Fig. 6h) and *Aubignyna perlucida* (Heron-Allen and Earland), whereas the allochthonous association was formed by *Bucella granulata* (Di Napoli), *Ammonia beccarii beccarii* (Lin.), *Elphidium crispum* (Lin.), *Asterigerinata mamilla* (Williamson), *Lobatula lobatula* (Walter and Jacob), *Quinqueloculina vulgaris* (D'Orbigny), *Q. bicornis* (Walter and Jacon), *Triloculina trigonula* (Lamarck), *Rosalina globularis* (Cushman), *Nonion commune* (D'Orbigny), *Adelosina laevigata* (D'Orbigny), *Elphidium complanatum* (D'Orbigni), *E. macellum* (Fitchel and Moll), *E. advenum* (Cushman) and Miliolidae. These species coincide with those described by Mateu (1989), Viñals *et al.* (1989) and Mateu *et al.* (1999) in the Pego-Oliva Basin record.

Several species of molluscs were identified in the cores of PDG7 and PDG2, including the gastropods *Cerithium* sp., *Cerithium vulgatum* (Bruguière), *Aporrhais pespelicani* (Linné) and the pelecypods, *Cardium* sp., *Pecten jacobaeus* (Linné), *Chlamys* sp., *Ostrea* sp., *Anomia epippium* (Linné), *Lima* cf. *lima* (Linné), *Ebala eulimoides* (Feki), *Manglia* sp. and *Donax* cf. *trunculus* (Linné). The pelecypod *Cerastoderma glaucum* (Poiret) (Fig. 6a) was present in all levels and *Scrobicularia plana* (da Costa) (Fig. 6b) was found in many samples, reflecting, together with other fauna, brackish environments.

Samples in PDG7 and PDG2 containing marine fossils (molluscs, ostracodes and/or autochtonous foraminifera) are shown in Figures 4 and 7.

n-*Alkanes*

Marshlands receive organic matter from both autochthonous (e.g. phytoplankton, bacteria and aquatic macrophytes) and allochthonous sources (e.g. terrestrial plant debris and pollen), and so environmental changes affecting the plant distribution are reflected in the biogeochemistry of sediments, although no specific differentiations can be recognized. In this regard, biomarkers contribute to the reconstruction of palaeoenvironmental conditions from marine and continental records (Meyers & Ishiwatari 1993; Meyers 1997, 2003). Sometimes the interpretation is not simple because, in most cases, organic matter is a mixture of components from many sources and with variable degrees of preservation. Despite diagenesis and alteration of the original organic matter when

sinking, sedimentary organic matter retains key information about its origin, and about how it was delivered and deposited (Meyers 2003). Within organic compounds, *n*-alkanes are among the biomarkers most commonly used. This is attributable to the fact that these compounds are less susceptible to microbial degradation than most types of organic molecules because they lack the functional groups that confer chemical reactivity, and they also have low water solubility (Prahl & Carpenter 1984; Meyers *et al.* 1995). These compounds retain key information about the origin of the organic matter and about how it was delivered and deposited (Meyers 2003). The *n*-alkanes present in sediments reflect mainly the contribution from algae, aquatic macrophytes and land plants. Several *n*-alkane ratios can be used for palaeoenvironmental reconstruction (Table 6).

The samples in the Pego-Oliva record (PDG7 and PDG2 cores) showed *n*-alkanes with an odd-over-even carbon number predominance, with a chain length distribution ranging mainly from C_{15} or C_{17} to C_{31} or C_{33}. This dominance is typical of non-mature organic matter from young sediments.

In order to handle the large number of data, we independently performed a multivariate analysis and a cluster analysis of data from the PDG7 and PDG2 boreholes. These analyses were carried out to establish the *n*-alkane indexes for each core, shown in Figure 7. For this purpose, we selected the terrigenous/aquatic ratio (TAR_{HC}) ratio, as an indicator of organic matter origin (algal v. terrestrial), the aquatic proxy (*Paq*) ratio, as a proxy for lake-level oscillations, and the relative percentages of C_{27}, C_{29} and C_{31} with respect to the sum $C_{27} + C_{29} + C_{31}$, which are linked to the amount of deciduous trees and grass inputs.

The two boreholes showed a high inverse correlation between the relative percentages of C_{27} and C_{31} (Tables 7 & 8), which may be related to wet–dry phases. The relative percentage of C_{29} was not associated with the relative percentage of C_{27} but showed a certain negative correlation with the percentage of C_{31} (correlation coefficients of -0.34 in PDG7 and -0.43 in PDG2: Tables 7 & 8). These results suggest that contribution of C_{29} was related not only to the presence of conifers (in which C_{29} dominates) but also to the variations of grass assemblages.

Of note, the *Paq* ratio, a proxy for aquatic macrophytes v. terrestrial plant input, in the two boreholes showed an inverse correspondence with the TAR_{HC} ratio, meaning that the algal contribution was generally linked to an increase in macrophyte input.

In PDG7 there was a negative covariation between the TAR_{HC} ratio and the relative percentage of C_{27}, thereby suggesting that, in some

Table 6. *Information provided by the* n-*alkane ratios*

n-Alkane ratio	Information
Predominant *n*-alkane chain	Indicator of the origin of the organic debris input: phytoplankton and algae are dominated by low molecular weight *n*-alkanes, maximizing at C_{17} (Gelpi *et al.* 1970; Blumer *et al.* 1971; Cranwell *et al.* 1987); submerged/floating macrophytes maximize at C_{21}, C_{23} and C_{25} (Cranwell 1984; Ogura *et al.* 1990; Viso *et al.* 1993); high molecular weight *n*-alkanes are dominant in terrestrial vascular plants ($>C_{25}$), maximizing at C_{27}, C_{29} and C_{31} (Cranwell *et al.* 1987)
Terrigenous/aquatic ratio – TAR_{HC} $(C_{27} + C_{29} + C_{31}/C_{15} + C_{17} + C_{19})$	Discriminates between the land plant (high values) and algal (low values) inputs (Silliman *et al.* 1996; Bourbonniere & Meyers 1996; Tenzer *et al.* 1999)
Aquatic proxy (*Paq*) $(C_{23} + C_{25}/C_{23} + C_{25} + C_{29} + C_{31})$	A proxy to determine the input of submerged/floating aquatic macrophyte relative to the emergent and terrestrial plant input (Ficken *et al.* 2000). $Paq < 0.1$ is linked to a considerable contribution from terrestrial plants; $Paq = 0.1–0.4$ reflects the relevant development of emergent macrophytes; $Paq > 0.4$ indicates a major input of submerged/floating macrophytes
Relative percentage of C_{27}, C_{29} and C_{31} *n*-alkanes with respect to the sum $C_{27} + C_{29} + C_{31}$	C_{27} enrichment is attributed to colonization by deciduous trees and, therefore, the presence of more humid conditions. In contrast, large amounts of C_{31} in sediments are associated with dry phases, with the development of extensive grass cover and pines. Conifers, especially pines, are rich in the C_{29} homologue, but also show a considerable C_{31} content (cf. Schwarcz *et al.* 2002; Ortiz *et al.* 2004*a*, 2010).

Table 7. *Correlation coefficients and significant levels between the Paq ratio, TAR_{HC}, and the relative percentages of C_{27}, C_{29} and C_{31} n-alkanes with respect to the sum $C_{27} + C_{29} + C_{31}$ in PDG7*

	TAR_{HC}	$\%C_{27}$	$\%C_{29}$	$\%C_{31}$
Paq	−0.54	0.27	−0.10	−0.21
	$p < 0.05$	$p = 0.8$	$p = 0.51$	$p = 0.18$
TAR_{HC}		−0.34	0.09	0.28
		$p < 0.05$	$p = 0.56$	$p = 0.07$
$\%C_{27}$			−0.19	−0.86
			$p = 0.21$	$p < 0.05$
$\%C_{29}$				−0.34
				$p < 0.05$

cases, the increase in algal input was linked to humid conditions. In PDG2, *Paq* values show a good correspondence with the relative percentage of C_{27}, implying that a rise in water input produced an increase in the water level of the marsh with the development of submerged macrophytes. Therefore, different conditions developed in distinct parts of the Pego-Oliva Basin.

A cluster analysis (complete linkage and Euclidean distance) performed on the TAR_{HC} ratio, *Paq* ratio and the relative percentage of C_{27} with respect to the sum $C_{27} + C_{29} + C_{31}$ differentiated six groups in PDG7 and five in PDG2 (Table 8). The mean values of the *n*-alkane ratios for each group are shown in Table 9. We did not include the relative percentages of C_{29} and C_{31} in the cluster analysis because the high correlation coefficients between these ratios and the relative percentage of C_{27} make this information redundant.

Group 1 represents the 'most aquatic' environment, as inferred from the lowest value of TAR_{HC} and the highest *Paq*, indicating phases with substantial algal and aquatic macrophyte contributions. The following groups until group 6 (PDG7) and group 5 (PDG2) represent gradually changing conditions to more terrestrial ones (higher input of terrestrial plants). Thus, samples of groups 3 and 4 are linked to a mixed contribution of algal and terrestrial plants, although the contribution of deciduous trees ($\%C_{27}$) varied. The groups defined in the two boreholes are aligned in Table 9 on the basis of their relative similarity.

Table 8. *Correlation coefficients and significant levels between the Paq ratio, TAR_{HC}, and the relative percentages of C_{27}, C_{29} and C_{31} n-alkanes with respect to the sum $C_{27} + C_{29} + C_{31}$ in PDG2*

	TAR_{HC}	$\%C_{27}$	$\%C_{29}$	$\%C_{31}$
Paq	−0.54	0.51	−0.23	−0.33
	$p < 0.05$	$p < 0.05$	$p = 0.21$	$p = 0.07$
TAR_{HC}		0.03	0.21	0.25
		$p = 0.14$	$p = 0.98$	$p = 0.17$
$\%C_{27}$			−0.19	−0.81
			$p = 0.30$	$p < 0.05$
$\%C_{29}$				−0.43
				$p < 0.05$

Of note, in all groups from PDG7 there was a visibly higher presence of caducifolia-derived alkanes (C_{27}) than in PDG2. Also, the values of $\%C_{27}$ in the groups did not show a clear correspondence with TAR_{HC} or *Paq* values (higher $\%C_{27}$ values were obtained in PDG7-III), meaning that the characteristics of the terrestrial plants varied, with a higher C_{27} homologue content during more humid periods. The palaeogeography of the marsh and variations in the water-table elevation, sedimentological conditions and sea level played an important role in determining the conditions of the marsh. On the basis of this interpretation, we classified each sample according to the cluster number to which it belonged and we constructed an *n*-alkane index log for each borehole (Fig. 7).

Interpretation and discussion

Sedimentology and stratigraphy

The amino acid chronology of PDG2, PDG3 and PDG7 allowed us to establish a correlation between these cores based on marine isotopic stages (MISs), which was tentatively extended to the other four cores. The assignment of the various MISs (Fig. 4) was established from the age–depth equations for the PDG2, PDG3 and PDG7 cores (Fig. 5) based on AAR datings, which were further used for the palaeoenvironmental reconstruction. Topographic levelling of the boreholes was not necessary as the largest difference between their elevations was 2 m (Table 1). The fence correlation (Fig. 4) of the records from the seven boreholes drilled in the Pego-Oliva marsh gives a general view of the basin geometry and completes the study of Viñals (1996). The sedimentation rates obtained for the PDG2, PDG3 and PDG7 cores indicate that the rate was markedly lower in PDG3 than in the others. In our view, the geometry of the basement, faulted in blocks (Fig. 1) (Viñals 1996 and confirmed by Ballesteros Navarro *et al.* 2009), reflects differential subsidence (Fig. 3). The lithostratigraphic correlation between PDG5 and PDG6 is rather uncertain because of the highly variable sedimentation on alluvial fans proximal to the sierras, and no numerical ages were obtained.

The high correlation coefficients of the age–depth functions in the dated cores also imply that, during the calculated time span of active sedimentation in the Pego-Oliva Basin, no major stratigraphical hiatuses occurred. Moreover, there was a

Table 9. *Mean values of the TAR_{HC} ratio, Paq ratio, and the relative percentage of the alkane C_{27} within the six groups identified in PDG7 and the five groups established in PDG2 from the cluster analysis*

	Group means for PDG7						Group means for PDG2				
	PDG7-I	PDG7-II	PDG7-III	PDG7-IV	PDG7-V	PDG7-VI	PDG2-I	PDG2-II	PDG2-III	PDG2-IV	PDG2-V
Paq	0.52	0.46	0.35	0.38	0.33	0.28	0.44	0.28	0.22	0.20	0.13
TAR_{HC}	1.76	2.48	2.70	4.09	7.14	28.57	2.48	3.47	4.55	12.42	28.50
C_{27} (%)	48.29	38.47	64.01	32.14	20.53	31.12	43.64	25.49	16.49	16.49	22.33

clear linear distribution of age (Asp D/L values) against depth for the PDG2, PDG3 and PDG7 cores. Should such major hiatuses have occurred, mainly during lowstand sea-level stages, the D/L values (or age equivalents) would appear as a staircased arrangement with plateaus in an age–depth plot marking the lack of sedimentation. Nevertheless, an unknown number of minor hiatuses occurred (caliche beds in some boreholes), but they were not detectable by AAR owing to a series of error sources linked to this method, including analytical preparation, sample errors and taphonomy. In the most unfavourable cases (raised beach deposits), the method clearly allowed identification of MIS (Hearty 1986, 1987; Hearty *et al.* 1986; Torres *et al.* 2000, 2010), thus it is difficult when major hiatuses with a time span comparable to that of a MIS interval occurred. These age–depth functions and the differential subsidence found between PDG7 and PDG3 are consistent with the subsidence rates calculated in Viñals (1996). There are only scarce data available to establish a comparison with the Pego-Oliva Basin, but some information on Jávea Bay, to the south of our study area and where Rey & Fumanal (1996*b*) calculated a subsidence ratio of $0.45\ m\ ka^{-1}$, supports the palaeoenvironmental evolution interpreted here.

On the basis of the lithologies observed in the Pego-Oliva record, we interpreted the facies and facies associations, which complete those of Viñals (1996), as follows.

The alluvial ('riverine') influence linked to alluvial fans was represented by gravels (G), sands (Sa – probably channelled deposits), and brown lutites (Fmy) and sandy lutites (Sa-Fmy) from the alluvial plain (alluvial-fan facies association). The brown sands and sandstones with very scarce unidentifiable bioclasts could correspond to fluvial deposits of low-energy streams (Sa). Their association with Fmy lithology was interpreted as alluvial plain and alluvial-plain-related ponds. These lutites contained variable amounts of ostracodes (*C. torosa*) and foraminifers (*A. beccarii*), and only a couple of samples were sterile.

Anoxic bottoms and high productivity are documented by grey/black fine-grained sediments (Fmb), which were interpreted as deposited in a marsh, fitting the definition of a salt-marsh provided by Adam (1993). These sediments sometimes showed a high presence of plant debris, constituting a peatland. Thus, peat deposits (F) correspond to wetland patches where emergent plants thrived or water-weed debris accumulated (fen and swamp facies association).

Fmb and Fmy corresponded to a low-energy environment and present a very limited variety of fossil genera. In fact, the macrofossil associations can be described as paucispecific, being dominated by *C. glaucum*, *S. plana* and, in some beds, large amounts of *Cerithium* sp. The *C. glaucum*–*Cerithium* sp. association is still present in brackish-water ponds some kilometres from the Mediterranean Sea. The microfossil association is overwhelmingly dominated by the *C. torosa* and *A. beccarii* association.

Fmb corresponded to high biological productivity and relatively anoxic bottoms, but the reproductive success of the biological association appeared to be ensured as attested by the abundance of spats and siblings of *C. glaucum*. In Fmy deposits, high biological productivity also took place but the water bottom was oxic or changed during emersion periods. However, according to Boyden & Russell (1972), the presence of *C. glaucum* attests a well wave-protected environment.

Fmb corresponded to a lagoonal environment in the Pego-Oliva Basin, from a seawater influence (saline marsh-lagoon facies) to brackish-water conditions dominated by the absence of a marine influence (brackish marsh facies). Full marine conditions (infralittoral) were never reached, but in some horizons there are some fossil remains that undoubtedly point to a marine influence. These shells were, in most cases, broken and deeply abraded (such as *Aporrhais pespelicani*, *Cerithium* sp. and *Ostreidae* indet.) and belonged to species usually inhabiting the infralittoral zone. They were washed onto the beach and were wave-abraded, and finally transported to the protected lagoon

zone during heavy storms. Fmy probably corresponds to a brackish-water temporary pond that is probably saline spring/river-fed (brackish marsh).

In some cases, oxygen reached the bottom, and yellow-white carbonate-rich layers (marls, marly limestones and limestones) were deposited. We interpret these carbonate deposits (M) as palustrine, with the depth of the water body probably not being very high (brackish palustrine facies). Some beds representing palustrine episodes were useful for correlation purposes, as identified in various boreholes (Fig. 4).

The input of waters with high salinities would have changed the water of the marsh/lagoon drastically from brackish to saline. This change did not need direct seawater entry into the marsh/lagoonal environment, at least during high sea-level periods, but severe droughts and the feeding by saline springs could have produced the higher salinity waters in the marsh (Cann & De Deckker 1981).

The black sands from the top of the records have a dominant littoral character (Sb): beach-barrier/back-barrier facies association. It is evident that some of these sediments correspond to a back-barrier environment: there, reworked beach and dune sands and bioclasts settled in an organic matter-rich sediment environment, and these materials were covered with a thin black film made of organic material (carbonaceous film). However, clean clasts (angular)/bioclasts (rounded) attest that this did not happen all of the time, and near the back-barrier small peat patches probably developed interfingering with sands. The core recovery process mixed sand beds.

Based on these considerations, the different facies associations of the seven boreholes shown in a fence diagram (Fig. 4) indicate varying palaeoenvironmental conditions. The PDG1 and PDG2 boreholes are almost identical and show a good correspondence of lithologies. PDG5, PDG6 and PDG4 were situated near the sierras where small alluvial fans developed, as attested by the presence of gravel and fine-grained sediments linked to the fan-toe (Fig. 1). The chronologies also allow us to confirm that there is a correlation between some palustrine/lacustrine episodes (marked with a P on Fig. 4) of white carbonate beds (marls and limestones).

The correlation of the boreholes based on the chronological framework allowed us to observe facies, fossils and biomarker associations. These, in turn, allowed us to establish the records of various palaeonvironmental patterns in the Pego-Oliva Basin, as discussed later (Fig. 8).

Biomarkers are commonly used for palaeoenvironmental reconstructions, although their use to ascertain the arrival or disappearance of certain plant species is not possible and comparison with pollen records is required. However, this region showed poor pollen remains (Fumanal & Dupré 1986). Notwithstanding, the *n*-alkanes provide information about the contribution of the main groups of vegetation to sediments: algal, aquatic macrophytes and land plants (Table 6), and in most cases these compounds are used as indirect approaches to define palaeoclimate in terms of water availability and moisture.

We chose to use a restrictive biofacies interpretation because almost all of the macro- and microfossil species showed a marked euryhaline character, in such a way that almost the entire record corresponds to a brackish lagoonal environment. The fence age correlation reveals a very complex palaeolandscape with channels (Sa, G), alluvial-plain fine-grained deposits (Fmy), and marshes covered by dominantly brackish water with high organic productivity (plants, and paucispeciphic shell beds) and partially anoxic bottoms where molluscs thrived (Fmb).

Clear marine inputs seem to be scarce and we considered it to be present where marine mollusc shells appear (Fig. 4), these being transported to the marsh zone during storms in periods of high-stand sea level, namely in odd MISs (MIS 15, MIS 11, MIS 10–MIS 9 boundary and MIS 5), although they also appear in some even MISs (MIS 14, MIS 6 and MIS 4). However, with two exceptions, these shells occur near the boundary with the overlying odd MIS and could be explained through uncertainties of AAR dating ages. In PDG7, there are clear marine representatives during the AAR-dated MIS 4. This information correlates well with the marine influence postulated by Mateu (1989). These monotonous environmental conditions in the upper part of the record were first mentioned by Mateu (1989), but Viñals (1996) identified a wider number of subenvironments that, on the basis of the lithofacies and biofacies, were very difficult to establish and, more importantly, the Pego-Oliva Basin was never in an infralittoral environment.

Thus, this interpretation of the terrestrial (brackish) character of the Pego-Oliva Basin infill can explain the abundance of biomarkers derived from upper plants and trees. In fact, Dupré *et al.* (1988) indicate that during some periods in the Late Pleistocene the coastline was 7–10 km further east of its present-day position. This observation would explain the considerable terrestrial-plant contribution to the Pego-Oliva Basin.

Palaeoenvironmental reconstruction

The oldest materials appeared in PDG7 and consisted mainly of grey, fine-grained carbonate lutites (Fmb) covering a time span of between

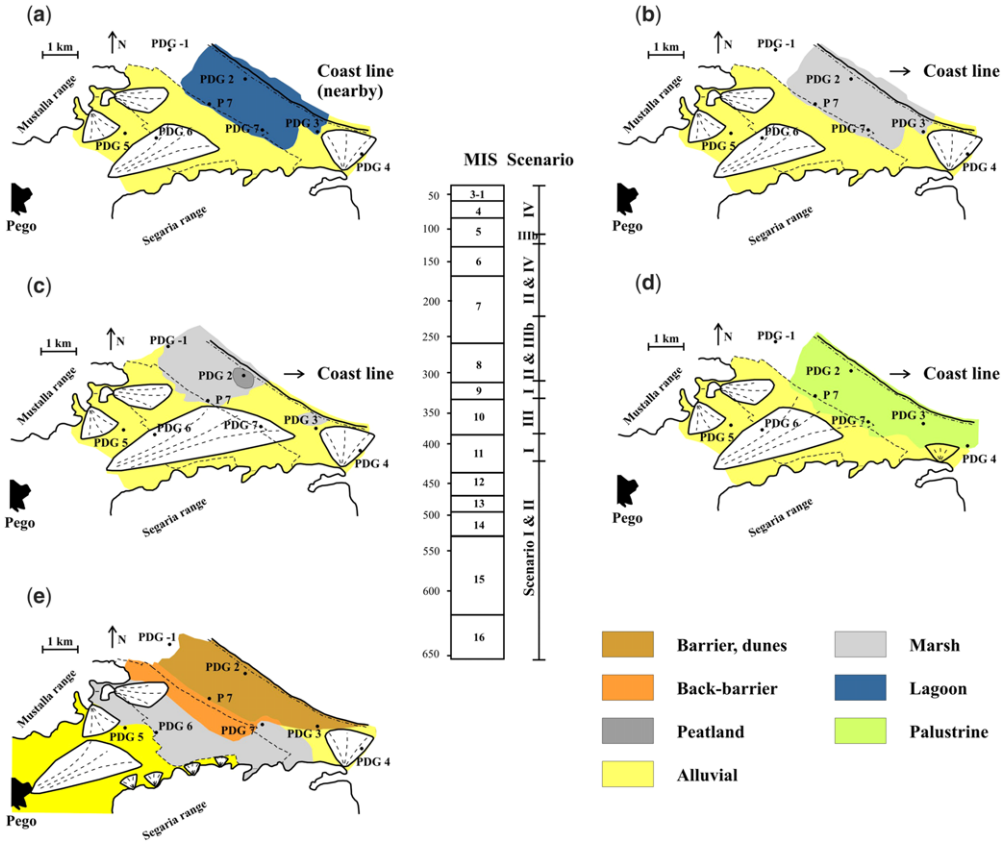

Fig. 8. Sketches diagrams of the main palaeogeogaphical scenarios interpreted in the Pego-Oliva Basin. (**a**) Sketch diagram (I) Alluvial saline marsh/lagoon-dominated (barrier offshore). (**b**) Sketch diagram (II) Alluvial-brackish marsh. (**c**) Sketch diagram (III) Alluvial-fan-dominated (local brackish marsh with episodic peatland deposits). (**d**) Sketch diagram (IIIb) Short lacustrine event. (**e**) Sketch diagram (IV) Present-day, beach, barrier, backshore, brackish marsh, alluvial fans.

about 620 and 460 ka (from MIS 15 to the MIS 12–MIS 11 boundary). On the basis of the fossil content (macrofossils and presence/absence of marine microfossils) and biomarkers, we interpreted a series of episodes with marine influence, in which algae and aquatic macrophytes increased, alternating with periods in which brackish waters were dominant (saline marsh-lagoon and brackish lagoon). The dominant fine-grained sedimentation of black-grey lutites indicated reducing bottoms and high biological productivity, and the almost constant presence of the *C. glaucum*, *C. torosa*, *A. beccarii* and *S. plana* association precludes anoxic conditions in some horizons with marcasite and fully pyritized phytoclasts. These observations thus indicate the presence of sulphate-reducing bacteria.

During the middle part of MIS 15 there was a dominance of samples belonging to the group 5 *n*-alkane group in PDG7, thereby indicating a terrestrial plant input, although samples at the beginning and the end of this stage showed a dominance of aquatics (group 1), which, together with the fossil content, indicates a marine influence. During MIS 14 there was a mixed terrestrial–aquatic plant input, with a slight decrease in the algae and aquatic input, in only one case did freshwater fauna, including charophytes (Fig. 6e), occur, indicating a decrease in the marine influence or a direct fluvial transportation from inland areas. During MIS 13, the aquatic input became the most important one (group 1). During MIS 12, terrestrial plants were abundant, indicating the dominance of terrestrial conditions, although brackish-water conditions remained. However, a brief pulse with a certain marine influence occurred at the end of MIS 12. In PDG2, dark lutites (Fmb) also occurred, as well as a dominance of plant biomarkers. At the end of MIS 12, a peatland developed.

Between 440 and 230 ka (MIS 11–MIS 7 *pro parte*) the wetland bottoms became oxic (yellow-brown sediments – lithologies Fmy, Sa and M) in PDG7, and sands and lutites linked to the probable progradation of the Pego alluvial fan accumulated, although brackish-water conditions prevailed (Fig. 7). The fossil content was markedly impoverished, but the ostracode *C. torosa* (which inhabits waters with a wide range of salinities) was common, while the pelecypod *C. glaucum* was scarce. Caliche (noduli) and root casts indicated short aerial exposure. The *n*-alkane indexes were from groups 1 and 2, indicating an increase in the algae and aquatic plant input at the expense of terrestrial plants, these conditions extending until the beginning of MIS 7. There was an alluvial-fan progradation, which was also recorded in PDG3 (Fig. 4). In contrast, the environmental conditions interpreted from PDG2 differed and deposits of Fmb continued (Fig. 7), with organic matter from terrestrial plants predominating (*n*-alkane index groups 3–5), except for MIS 8 when aquatic input dominated (group 1). During MIS 11, MIS 9–MIS 8 boundary and MIS 7, there were some episodes in which marine fossils were recorded, associated with grey lutites, these probably linked to highstand sea levels. At the end of MIS 12, caliche beds developed and near the top of this interval, in PDG2 (MIS 7), peat accumulated (P), implying that this area sporadically and locally acted as a pond. However, these deposits were not thick and appeared together with allochthonous marine microfossils.

In the middle part of MIS 7 (*c.* 230–200 ka) there was a change towards Fmb lithologies, with *C. glaucum* and biomarkers from aquatic plant provenance (groups 1 and 2) in PDG7. The sporadic presence of pyrite/marcasite was observed. These conditions changed sharply to a more terrestrial plant input (group 6), with light lutites (Fmy), thus indicating oxic bottoms. However, in PDG2, brackish to saline conditions occurred in a short pulse with stagnant waters, which was followed by yellow fine-grained sands interpreted to be back-barrier deposits, although the recovery of this interval was poor. Changes in lateral facies explain the distinct palaeoenvironments recorded in PDG7 and PDG2 (Fig. 8).

In MIS 6 (180–130 ka) there was an important terrestrial influence, the algal and aquatic input being markedly reduced (group 6), being especially noticeable in PDG2, with the presence of non-marine fauna. In our view a brackish marsh, fed mainly by aquifers and rivers, existed that was little affected by marine processes.

It is noticeable that the MIS 6–MIS 5 boundary in PDG7 (*c.* 140–130 ka) was marked by a short palustrine/lacustrine event (Fig. 7), which was characterized by the abundance of ostracodes. This finding is consistent with the palustrine event identified by Dupré *et al.* (1988) in the P7 borehole at the same depth.

In both PDG7 and PDG2, MIS 5 (*c.* 130–80 ka) began with black lutites followed by marine sands (Sb) with molluscs, ostracodes and forams. Algae and aquatic plant-derived biomarkers dominated towards the top, and it is noticeable that in PDG2 the presence of terrestrial plant biomarkers coincided with a bed of peat (carbonaceous phytoclasts).

From the top of MIS 5 to the end of the record (80 ka–Present), it was not possible to clearly distinguish the stage boundaries because loose sands were slurried during drilling. According to Dupré *et al.* (1988), these were washover deposits, whereas Durán *et al.* (2005) reported that they were aeolian in origin. The most outstanding characteristics of these sands (Sb) are their excellent sorting, their medium grain size, and the presence of large amounts of bioclasts, namely shell fragments, abraded foram tests and others. Given the current faunal assemblage on beaches and the absence of wind-blown marine organisms in aeolian deposits, the hypothesis of washover accumulation is the most plausible explanation for the origin of these sediments. It seems that during this part of the record marine-influenced facies and algal origin *n*-alkanes prevailed, thus pointing to a palaeogeographical pattern with a back-barrier in the east of the study area that protected a saline–brackish marsh inwards (Viñals 1996).

The study of the Pego-Oliva Basin performed by Dupré *et al.* (1988) showed that pollen data are scarce. In fact, these data were significant only in the uppermost metres, reflecting the climate amelioration in the Holocene; but the deeper samples reflected only an aquatic environment. Those authors detected a stratigraphical hiatus between 11 and 15 m depth; however, we did not observe this through AAR dating, although only a few samples were studied in the uppermost metres.

In the Elx Bay zone, south of the Pego-Oliva Basin, Blázquez (2005) defined an almost continuous sedimentation period tentatively extending from MIS 12 to the Holocene: regressive periods were linked to the arrival of alluvial deposits during even MIS, and episodes with infralittoral conditions or lagoonal facies with marine influence during MIS 11, MIS 7 and MIS 5 corresponded to highstand sea-level periods. This coincides with the palaeoenvironmental conditions interpreted in the Pego-Oliva Basin, where facies with a marine influence were recorded in the same odd MIS (Fig. 7). Although alluvial-fan progradation was also observed in the Pego-Oliva record during even MIS, a continental brackish wetland developed, and there were some episodes in which some marine

influence occurred, which can be explained by the local neotectonic subsidence (Fig. 3). The uppermost part of the Elx Bay record consists of marine sands, coinciding with those observed in the Pego-Oliva Basin.

Similar to the Pego-Oliva Basin, in the Crotone Basin (Calabria, southern Italy) alluvial-fan progradation was observed in some cores during even MISs, whereas during odd MISs brackish–saline lagoonal deposits occurred (Capraro *et al.* 2011). In the Venetian Lagoon, alluvial deposits occurred in MIS 2, while a marine influence took place during the Holocene sea rise (Serandrei Barbero 1975; Favero & Serandrei Barbero 1980, 1983). Likewise, in the Apulian Tavoliere plain (southern Italy), De Santis *et al.* (2010) found lagoonal conditions with *Cerastoderma* sp. remains, and with alluvial-fan progradation especially during MIS 12, MIS 10, MIS 8 and MIS 6. Coinciding with De Santis *et al.* (2010), sea-level highstands were especially noticeable during MIS 11 and MIS 5, allowing the formation of marine terraces in the Mediterranean realm (Zazo 1999; Schellmann & Radtke 2004).

The marine conditions that developed during MIS 5 (although we were unable to differentiate MIS boundaries), even in PDG7, showed a good correspondence with transgressive conditions that produced the development of raised marine deposits along the Spanish Mediterranean coast (Hearty 1987; Hearty *et al.* 1986; Torres *et al.* 2000, 2010; Dabrio *et al.* 2011), and the coasts of Italy (Hearty 1986; Belluomini *et al.* 1986, 1993; Hearty *et al.* 1986), Morocco (Brückner 1986; Hearty 1986) and Tunisia (Hearty 1986; Miller *et al.* 1986). Similarly, the coastal area south of the province of Alicante hosts a lagoon (Santa Pola Lagoon) that has been separated from the open sea by coastal barriers since at least Middle Pleistocene times (Dabrio *et al.* 2011). Likewise, in the Jávea and Moraira bays, located 30 and 40 km south of the Pego-Oliva Basin, respectively, Fumanal *et al.* (1993*b*), Viñals (1995*a*, *b*) and Viñals & Fumanal (1995) recognized the presence of marine transgressive episodes during MIS 7 and MIS 5, whereas MIS 8 and MIS 6 corresponded to regressive phases characterized by the progradation of alluvial fans.

Conclusions

The abundance of the ostracode *C. torosa* in almost all of the beds of the cores studied allowed AAR dating of the Middle Pleistocene–Holocene record of the Pego-Oliva Basin, which covers approximately 650 ka (from MIS 15 to MIS 1). However, in the uppermost sands the most recent four MIS were only tentatively placed. A statistically significant lineal depth–age function was observed for three boreholes, demonstrating the lack of major (MIS interval) stratigraphical gaps, although local subsidence rate variations were detected from changes in the isochron slopes in PDG7 and PDG3, which affected the thickness and type of the deposits in different parts of the basin, and produced lateral changes in facies. The goodness of fit of the ages calculated through the racemization–age algorithm confirmed the previously published Holocene and Upper Pleistocene ages obtained through thermoluminescence and radiocarbon methods in samples from former Pego-Oliva boreholes (Dupré *et al.* 1988; Viñals & Fumanal 1995; Viñals 1996).

On the basis of the lithology and sedimentological characteristics, six lithofacies associations were distinguished, corresponding to beach/back-barrier deposits, saline marsh-lagoon, brackish marsh, brackish palustrine, fen/swamp (peatland) and alluvial-fan (fluvial) influence.

The use of organic geochemistry, namely the *n*-alkane content, which is extensively used in palaeoenvironmental reconstruction, was a useful tool to employ for the Pego-Oliva record. The statistical analysis of the *n*-alkane ratios allowed us to distinguish several environmental (plant–biomes) patterns. Our results reveal that there was a constant and considerable input of terrestrial plant-derived biomarkers to a shallow wetland, where the dominance of algae, submerged, floating or emergent macrophytes varied.

The Pego-Oliva Basin can be defined during most of its geological history as a brackish wetland, distally linked to alluvial fans in the western part, and to a low stepped platform to the east (Fig. 4). Sporadically quasi-lagoonal conditions developed and saline waters invaded the basin mainly during some odd MISs, although the biomarker input indicated that the terrestrial influence remained substantial. Only during short time periods did palustrine or peatland conditions appear. There is a good correspondence with other records in the western Mediterranean realm, although local conditions produced some differences, these were caused mainly by variations in subsidence rates.

Palaeogeography began with a clear alternation of brackish marsh–lagoon periods with anoxic conditions from MIS 15 to MIS 12 (palaeogeographical sketch diagrams I & II, Fig. 8).

During MIS 11–MIS 7, there was a clear alluvial influence (sands and brown lutites) in the western part of the basin (PDG3, PDG4 and some in PDG7). These deposits were not recorded in the PDG2 record, in which brackish marsh conditions prevailed, sometimes with peat accumulation (palaeogeographical sketch diagrams II and III, Fig. 8): However, some carbonate horizons of PDG7 and

PDG2 were correlated, marking brackish palustrine conditions (palaeogeographical sketch diagram IIIb, Fig. 8). During MIS 9, saline marsh–lagoon conditions occurred. Towards the basin boundary, alluvial fans were active as attested by gravel and sand deposits.

A following period with brackish marsh development and barrier deposits was confirmed in MIS 7 by the presence of black lutites with mollusc, foraminifer and ostracode associations, all of which hatched in the basin dominion (palaeogeographical sketch diagrams II and IV, Fig. 8). Afterwards, alluvial fans prograded (at the end of MIS 7–MIS 6) with a brackish marsh in the central part, and a palustrine event was interpreted in the MIS 6–MIS 5 boundary (palaeogeographical sketch diagram IIIb, Fig. 8).

During MIS 5–MIS 1, the palaeogeography of the Pego-Oliva Basin changed, with the presence of barrier sands in its northern dominion (PDG2) during highstand sea-level periods (Viñals & Fumanal 1995; Viñals 1996), whereas, in the central part (PDG7), a marsh was present (palaeogeographical sketch diagram IV, Fig. 8); this wetland remains active today.

In brief, here is provided the first complete palaeogeographical evolution of the Pego-Oliva Basin (Mediterranean coast, Iberian Peninsula). Using AAR, sedimentology, fossil content and biomarkers, a series of paleoenvironmental data was obtained for almost the whole of the Middle Pleistocene record. These data indicate that, in spite of variations in sea level, the terrestrial influence remained for a long time.

Funding was obtained through the project REM-100615 TDTPH. We thank Mr F. Montero, from the Spanish Geological Survey, who helped in the sampling of the boreholes. We thank Profs P. Martini, V. Pascucci, C. Murray-Wallace and an anonymous reviewer for their very helpful comments on the manuscript

References

Adam, P. 1993. *Saltmarsh Ecology*. Cambridge University Press, Cambridge.

Badal, E. & Roiron, P. 1995. La prehistoria de la vegetación en la Península Ibérica. *Saguntum*, **28**, 29–48.

Ballesteros Navarro, B. J., Ocaña, L., López, J. C. & Rodríguez, L. 2006. Contribución de las técnicas isotópicas y de las relaciones hidroquímicas al conocimiento de los mecanismos que rigen los procesos de salinización en un aquífero kástico litoral de la provincia de Alicante, España. *In*: Sánchez-Vila, X., Cabrera, M. C. & Valverde, M. (eds) *International Worshop from Data Gahering and Groundwater Modelling to Integrated Management*. Serie Hidrogeología y aguas subterráneas, **21**. Instituto Geológico y Minero de España, Madrid, 185–192.

Ballesteros Navarro, B. J., Domínguez Sánchez, J. A. & Díaz-Losada, E. 2008. *Resultados de los sondeos de investigación realizados en el marjal de Pego-Oliva*. Internal Report. Instituto Geológico y Minero de España, Madrid.

Ballesteros Navarro, B. J., Domínguez Sánchez, J. A., Díaz-Losada, E. & García Menéndez, O. 2009. Zonas húmedas mediterráneas y acuíferos asociados. Condicionantes hidrogeológicos del Marjal de Pego-Oliva (Alicante-Valencia). *Boletín Geológico y Minero*, **120**, 459–478.

Belluomini, G., Branca, M., Delitala, L., Pecorini, G. & Spano, C. 1986. Isoleucine epimerization dating of quaternary marine deposits in Sardinia, Italy. *Zeitschrift für Geomorphologie*, **62**, 109–117.

Belluomini, G., Manfra, L. & Proposito, A. 1993. Una recente aminocronologia dei depositi marini pleistocenici delĺarea di Montalto di Castro e Tarquinia (Viterbo). *Il Quaternario*, **6**, 241–248.

Blázquez, A. M. 2005. *Evolución cuaternaria de l'Albufera d'Elx: Paleoambientes y foraminíferos fósiles*. Memorias del Museo Paleontológico de Elche, **1**. Museo Paleontológico de Elche (MUPE), Alicante.

Blázquez, A. M. & Ferrer, C. 2003. L'Albufereta d'Alacant: foraminíferos y evolución paleoambiental. *Cuaternario y Geomorfología*, **18**, 55–72.

Blázquez, A. M. & Usera, J. 2010. Palaeoenvironments and Quaternary foraminifera in the coastal lagoon of Elx (Alicante, Spain). *Quaternary International*, **221**, 68–90.

Blumer, M., Guillard, R. R. L. & Chase, T. 1971. Hydrocarbons of marine plankton. *Marine Biology*, **8**, 183–189.

Bourbonniere, R. A. & Meyers, P. A. 1996. Sedimentary geolipid records of historical changes in the watersheds and productivities of Lakes Ontario and Erie. *Limnology and Oceanography*, **41**, 352–359.

Boyden, C. R. & Russell, P. J. C. 1972. The distribution and habitat range of a brackish water cockle *Cardium* (*Cerastoderma*) in the British Isles. *Journal of Animal Ecology*, **41**, 719–734.

Bright, J. & Kaufman, D. S. 2011. Amino acid racemization in lacustrine ostracodes, part I: effect of oxidizing pre-treatments on amino acid composition. *Quaternary Geochronology*, **6**, 154–173.

Burjachs, F. & Juliá, R. 1994. Abrupt climatic changes during the last glaciation based on pollen analysis of the Abric Romani, Catalonia, Spain. *Quaternary Research*, **42**, 308–315.

Brückner, H. 1986. Stratigraphy, evolution and age of quaternary marine terraces in Morocco and Spain. *Zeitschrift für Geomorphologie*, **62**, 83–101.

Cann, & De Deckker, P. 1981. Fossil quaternary and living foraminífera from athalassic (non-marine) saline lakes, Southern Australia. *Journal of Paleontology*, **55**, 660–670.

Cantoral, E. A. & Aboal, M. 2001. El Marjal Pego-Oliva: evolución temporal de la flora de macroalgas. *Limnetica*, **20**, 159–171.

Cantoral, E. A. & Aboal, M. 2008. Diatomeas (Baciariophyceae) del marjal Oliva-Pego (Comunidad Valenciana, España). *Anales Jardin Botanico de Madrid*, **65**, 111–128.

Capraro, L., Massari, F. *et al.* 2011. Chronology of the Lower-Middle Pleistocene succession of the south-western part of the Crotone Basin (Calabria, Southern Italy). *Quaternary Science Reviews*, **30**, 1185–1200.

Carbonel, P. & Pujos, M. 1982. Les variations architecturales des microfaunes du lac de Tunis: relations avec lenvironnement. *In*: Lasserre, P. & Postma, H. (eds) *Coastal Lagoons: Proceedings of the International Symposium on Coastal Lagoons*, Bordeaux, France, 8–14 September 1981. *Oceanologica Acta*, Special Issue, 79–85.

Carrión, J. S. 1992. A palaeoecological study in the western Mediterranean area. The Upper Pleistocene pollen record from Cova Beneito (Alicante, Spain). *Palaeogeography, Palaeoclimatology, Palaeoecology*, **92**, 1–14.

Carrión, J. S. & Dupré, M. 1996. Late Quaternary vegetational history at Navarrés, eastern Spain. A two core approach. *New Phytologist*, **134**, 177–199.

Carrión, J. S. & Munuera, M. 1997. Upper Pleistocene palaeoenvironmental change in Eastern Spain: new pollen-analytical data from Cova Beneito (Alicante). *Palaeogeography, Palaeoclimatology, Palaeoecology*, **128**, 287–299.

Carrión, J. S. & van Geel, B. 1999. Fine-resolution Upper Weichselian and Holocene palynological record from Navarrés (Valencia, Spain) and a discussion about factors of Mediterranean forest succession. *Review of Palaeobotany and Palynology*, **106**, 209–236.

Carrión, J. S., Dupré, M., Fumanal, M. P. & Montes, R. 1995. A palaeoenvironmental study in the semi-arid southeastern Spain: the palynological and sedimentological sequence at Perneras Cave (Lorca, Murcia). *Journal of Archaeological Science*, **22**, 355–367.

Carrión, J. S., Munuera, M., Navarro, C., Burjachs, F., Dupré, M. & Walker, M. J. 1999. The palaeoecological potential of pollen records in caves: the case of Mediterranean Spain. *Quaternary Science Reviews*, **18**, 1061–1073.

Causse, Ch., Goy, J. L., Zazo, C. & Hillaire-Marcel, C. 1993. Potential chronologique (Th/U) des faunes Pléistocenes Mediterranéennes: example des terracesses marines des regions de Murcie et Alicante (South-Est de l'Espagne). *Geodinamica Acta*, **6**, 121–134.

Champetier, Y. 1972. *Le Prebetique et l'Ibèrique cotiers dans le Sud de la Province de Valence et le Nord de la Province d'Alicante (Espagne)*. PhD thesis, University of Nancy.

Collado, M. A. & Robles, F. 1983. Estudio de las asociaciones de moluscos de la turbera holocena de Torreblanca (Castellón). *Mediterránea Serie Geológica*, **1**, 105–142.

Cranwell, P. A. 1984. Lipid geochemistry of sediments from Upton Broad, a small productive lake. *Organic Geochemistry*, **7**, 25–37.

Cranwell, P. A., Eglinton, G. & Robinson, N. 1987. Lipids of aquatic organisms as potential constributors to lacustrine sediments-II. *Organic Geochemistry*, **11**, 513–527.

Dabrio, C. J., Zazo, C. *et al.* 2011. Millennial/submillennial-scale sea level fluctuations in western Mediterranean during the second highstand of MIS 5e. *Quaternary Science Reviews*, **30**, 335–346.

De Deckker, P. 1981. Ostracods of athalassic saline lakes. *Hydrobiologia*, **81**, 131–144.

De Santis, V., Caldara, M., Torres, T. & Ortiz, J. E. 2010. Stratigraphic units of the Apulian Tavoliere plain (Southern Italy): chronology, correlation with marine isotope stages and implications regarding vertical movements. *Sedimentary Geology*, **228**, 255–270.

Díaz del Río, V., Rey, J. & Vegas, R. 1986. The Gulf of Valencia continental shelf: extensional tectonics in Neogene and Quatemary sediments. *Marine Geology*, **73**, 169–179.

Dumas, B. 1977. *Le levant Espagnol: la genèse du relief*. PhD thesis, Politechnical University of Paris-Sorbonne.

Dupré, M., Fumanal, M. P., Sanjaume, E., Santisteban, C., Usera, J. & Viñals, M. J. 1988. Quaternary evoltion of the Pego coastal lagoon (Southern Valencia, Spain). *Palaeogeography, Palaeoclimatology, Palaeoecology*, **68**, 291–299.

Durán, J. J., García de Domingo, A., López Geta, J. A., Robledo, P. A. & Soria, J. M. 2005. *Humedales del Mediterráneo Español: modelos geológicos e hidrogeológicos*. Hidrogeología y Aguas Subterráneas, **3**, Instituto Geológico y Minero de España (IGME), Madrid.

Egidos, A. I. & Aboal, M. 2003. *Thorea violacea* Bory de Saint-Vincent (Thoreacea, Rodophyceae) en una surgencia del Marjal Pego-Oliva (Comunidad Valenciana). Nueva cita para la flora algal española. *Anales Jardín Botánico Madrid*, **60**, 27–32.

Favero, V. & Serandrei Barbero, B. 1980. Origene ed evoluzione della laguna di Venezia (Bacino meridionale). *Lavori Società Veneziana di Scienze Naturali*, **5**, 49–71.

Favero, V. & Serandrei Barbero, B. 1983. Oscillazione del livello marino ed evoluzione paleoambientalle della laguna di Venezia nell'area compresa tra Torcello ed il margine lagunare. *Lavori Società Veneziana di Scienze Naturali*, **8**, 83–102.

Ferrer, C., Blázquez, A. M., Esquembre, M. A. & Ortega, J. R. 2005. Reconstrucción paleoambiental de l'Albufereta d'Alacant durante el período ibero-romano (500 A.C.–300 D.C.). *In*: Sanjaume, E. & Mateu, J. F. (eds) *Geomorfologia litoral i Quaternari, Homenatge al Professor Vicenç M. Rosselló i Verger*, Universidad de Valencia, Valencia, 137–150.

Ficken, K. J., Li, B., Swain, D. L. & Eglinton, G. 2000. An *n*-alkane proxy for the sedimentary input of submerged/floating freshwater aquatic macrophytes. *Organic Geochemistry*, **31**, 745–749.

Fontes, J. Ch., Gasse, F., Callot, Y., Plaziat, J.-C., Carbonel, P., Dupeuble, P. A. & Kaczmarska, I. 1985. Freshwater to marine-like environments from Holocene lakes in northern Sahara. *Nature*, **317**, 608–610.

Fumanal, M. P. & Dupré, M. 1986. Aportaciones de la sedimentología y de la palinología al conocimiento del paleoambiente valenciano durante el Holoceno. *In*: López Vera, F. (ed.) *Quaternary Climate in Western Mediterranean*. Universidad Autónoma de Madrid, Madrid, 325–343.

FUMANAL, M. P., MATEU, G., REY, J., SOMOZA, L. & VIÑALS, M. J. 1993*a*. Las unidades morfosedimentarias cuaternarias del litoral del Cabo de la Nao (Valencia-Alicante) y su correlación con la plataforma continental. *In*: FUMANAL, P. & BERNABEU, J. (eds) *Estudios sobre Cuaternario. Medios Sedimentarios, cambios Ambientales, Habitat Humano*. Universidad de Valencia, Valencia, 53–64.

FUMANAL, M. P., USERA, J., VIÑALS, M. J., MATEU, G., BELLUOMINI, G. & PROSZYNSKA-BORDAS, H. 1993*b*. Evolución cuaternaria de la bahía de Xàbia (Alicante). *In*: FUMANAL, P. & BERNABEU, J. (eds) *Estudios sobre Cuaternario. Medios Sedimentarios, cambios Ambientales, Habitat Humano*. Universidad de Valencia, Valencia, 17–27.

GASSE, F., FONTES, J. C. *ET AL*. 1987. Biological remains, geochemistry and stable isotopes for the reconstruction of environmental and hidrological changes in the Holocene lakes from North Sahara. *Palaeogeography, Palaeoclimatology, Palaeoecology*, **60**, 1–46.

GELPI, E., SCHNEIDERA, H., MANNA, J. & ORÓA, J. 1970. Hydrocarbons of geochemical significance in microscopic algae. *Phytochemistry*, **9**, 603–612.

GOY, J. L. & ZAZO, C. 1974. Estudio morfotectónico del cuaternario en el óvalo de Valencia. *In*: *Actas de la I Reunión Nacional del Grupo de Trabajo del Cuatcrnario, Madrid*. Instituto Lucas Mallada (CSIC), Madrid, 71–82.

GOY, J. L., ZAZO, C. & HILLAIRE-MARCEL, C. 1986. Stratigraphie et chronologie (U/Th) du Thyrrénien du Sud-Est de l'Espagne. *Zeitschrift für Geomorphologie*, **62**, 71–82.

GUILLAUME, M. C., PEYPOUQUET, J. P. & TETART, J. 1985. Quaternaire et Actuel. *In*: OERTLI, H. J. (ed.) *Atlas des Ostracodes de France. Bulletin des Centres de Recherches Exploration–Production Elf-Aquitaine*, **9**, 337–377.

HARE, P. E. 1969. Geochemistry of proteins, peptids and amino acids. *In*: EGLINTON, G. & MURPHY, M. T. J. (eds) *Organic Geochemistry; Methods and Results*. Springer, New York, 438–463.

HEARTY, P. J. 1986. An Inventory of Last Interglacial (sensu lato) Age Deposits from the Mediterranean Basin. *Zeitschrift für Geomorphologie*, **62**, 51–69.

HEARTY, P. J. 1987. New data on the Pleistocene of Mallorca. *Quaternary Science Reviews*, **6**, 245–257.

HEARTY, P. J., MILLER, G., STEARNS, C. & SZABO, B. J. 1986. Aminostratigraphy of Quaternary shorelines in the Mediterranean basin. *Geological Society of America Bulletin*, **97**, 850–858.

HEARTY, P. J., O'LEARY, M. J., KAUFMAN, D. S., PAGE, M. & BRIGHT, J. 2004. Amino acid geochronology of individual foraminifer (*Pulleniatina obliquiloculata*) tests, north Queensland margin, Australia: a new approach to correlating and dating Quaternary tropical marine sediment cores. *Paleoceanography*, **19**, PA4022, http://dx.doi.org/10.1029/2004PA001059.

HERNÁNDEZ RUIZ, M., DEL VAL, J. & VIÑALS, M. J. 1993. Aplicación de técnicas geofísicas al estudio del Cuaternario: prospección geoeléctrica mediante S.E.V. en el Marjal de Oliva-Pego (Valencia-Alicante). *Cuaternario y Geomorfología*, **7**, 79–90.

HILLAIRE-MARCEL, C., CARRO, O., CAUSSE, Ch., GOY, J. L. & ZAZO, C. 1986. Th/U dating of *Strombus bubonius* bearing marine terraces in southeastern Spain. *Geology*, **14**, 613–616.

KAUFMAN, D. S. 2000. Amino acid racemization in ostracodes. *In*: GOODFRIEND, G., COLLINS, M., FOGEL, M., MACKO, S. & WEHMILLER, J. (eds) *Perspectives in Amino Acid and Protein Geochemistry*. Oxford University Press, New York, 145–160.

KAUFMAN, D. S. & MANLEY, W. F. 1998. A new procedure for determining DL amino acid ratios in fossils using reverse phase liquid chromatography. *Quaternary Geochronology*, **17**, 987–1000.

MATEU, G. 1989. Sondeo de l'Albufera de Pego: micropaleontología y biofacies. *Cuadernos de Geografía*, **49**, 1–9.

MATEU, G., VIÑALS, M. J. & MOREIRO, M. 1997. Biofacies marginolitorales del Mediterráneo Occidental (Baleares, Valencia, Alicante y Murcia). *Boletín de la Sociedad de Historia Natural de Baleares*, **40**, 123–134.

MATEU, J. F., SANCHIS, C. & FERRI, M. 1999. El golf de Valéncia durant els segles XVI i XVII. Canvis ambientals. *In*: ROSSELLÓ, V. M. (ed.) *Geoarqueologia i Quaternari litoral. Memorial M.P. Fumanal*. Universidad de Valencia, Valencia, 367–374.

MEYERS, P. A. 1997. Organic geochemical proxies of paleoceanographic, paleolimnologic, and paleoclimatic processes. *Organic Geochemistry*, **27**, 213–250.

MEYERS, P. A. 2003. Applications of organic geochemistry to paleolimnological reconstructions: a summary of examples from the Laurentian Great Lakes. *Organic Geochemistry*, **34**, 261–289.

MEYERS, P. A. & ISHIWATARI, R. 1993. Lacustrine organic geochemistry-an overview of indicators of organic matter sources and diagenesis in lake sediments. *Organic Geochemistry*, **20**, 867–900.

MEYERS, P. A., LEENHEER, M. J. & BOURBONNIERE, R. A. 1995. Diagenesis of vascular plant organic matter components during burial in lake sediments. *Aquatic Geochemistry*, **1**, 35–42.

MILLER, G. H., PASKOFF, R. & STEARNS, C. E. 1986. Amino Acid Geochronology of Pleistocene Littoral Deposits in Tunisia. *Zeitschrift für Geomorphologie*, **62**, 197–207.

OGURA, K., MACHILARA, T. & TAKADA, H. 1990. Diagenesis of biomarkers in Biwa lake sediments over 1 million years. *Organic Geochemistry*, **16**, 805–813.

ORTIZ, J. E. 2000. *Evolución paleoclimática durante el Pleistoceno de la mitad sur de la Península Ibérica mediante el estudio paleontológico y geoquímico de ostrácodos de la cuenca de Cúllar-Baza (Granada, España)*. PhD thesis, Politechnical University of Madrid.

ORTIZ, J. E., TORRES, T., DELGADO, A., JULIÀ, R., LLAMAS, F. J., SOLER, V. & DELGADO, J. 2004*a*. Numerical dating algorithms of amino acid racemization ratios analyzed in continental ostracodes of the Iberian Peninsula (Spain). Application to Guadix-Baza Basin (southern Spain). *Quaternary Science Reviews*, **23**, 717–730.

ORTIZ, J. E., TORRES, T. *ET AL*. 2004*b*. The palaeoenvironmental and palaeohydrological evolution of Padul Peat Bog (Granada, Spain) over one million years,

from elemental, isotopic, and molecular organic geochemical proxies. *Organic Geochemistry*, **35**, 1243–1260.

ORTIZ, J. E., TORRES, T., JULIÀ, R. & LLAMAS, F. J. 2004*c*. Algoritmos de cálculo de edad a partir de relaciones de racemización/epimerización de aminoácidos en pelecípodos marinos del litoral mediterráneo español. *Revista de la Sociedad Geológica de España*, **17**, 217–227.

ORTIZ, J. E., TORRES, T. *ET AL*. 2010. Palaeoenvironmental changes in the Padul Basin (Granada, Spain) over the last 1 Ma based on the biomarker content. *Palaeogeography, Palaeoclimatology, Palaeoecology*, **298**, 286–299.

PÉREZ-OBIOL, R. & JULIA, R. 1984. Climatic change on the Iberian Peninsula recorded in a 30 000-yr pollen record from Lake Banyoles. *Quaternary Research*, **41**, 91–98.

PRAHL, F. G. & CARPENTER, R. 1984. Hydrocarbons in Washington coastal sediments. *Estuarine, Coastal and Shelf Science*, **18**, 703–720.

PULIDO, A. 1979. *Contribución al conocimiento de la hidrogeología del prebético nororiental*. Servicio de Publicaciones, Ministerio de Industria y Energía, Madrid.

REY, J. & FUMANAL, M. P. 1996*a*. Cuaternario submarino frente a la Serra Gelada (Alicante) y sus implicaciones eustático-paleogeográficas. *Cuadernos de Geografía*, **60**, 243–258.

REY, J. & FUMANAL, M. P. 1996*b*. The valencian coast (western Mediterranean): neotectonics and geomorphology. *Quaternary Science Reviews*, **15**, 789–802.

ROCA, J. R. & JULIÁ, R. 1997. Late-glacial and holocene lacustrine evolution based on ostracode assemblages in southeastern Spain. *Geobios*, **30**, 823–830.

RODRÍGUEZ ESTRELLA, T. 1977. Síntesis geológica del Prebético de la Provincia de Alicante 1) Estratigrafía. *Boletín Geológico y Minero*, **88**, 183–214.

RUEDA, J. & MÉZCUA, J. 2002. Estudio del terremoto de 23 de septiembre de 2001 en Pego (Alicante). Obtención de una relación mbLg-Mw para la Península Ibérica. *Revista Sociedad Geológica de España*, **15**, 159–173.

SALVANY, J. M., LARRASOAÑA, J. C., MEDIAVILLA, C. & REBOLLO, A. 2011. Chronology and tectonosedimentary evolution of the Upper Pliocene to Quaternary deposits of the lower Guadalquivir foreland basin, SW Spain. *Sedimentary Geology*, **241**, 22–39.

SCHELLMANN, G. & RADTKE, U. 2004. A revised morpho- and chronostratigraphy of the Late and Middle Pleistocene coral reef terraces on Southern Barbados (West Indies). *Earth-Science Reviews*, **64**, 157–187.

SCHWARCZ, L., ZINK, K. & LECHTERBECK, J. 2002. Reconstruction of postglacial to early Holocene vegetation history in terrestrial Central Europe via cuticular lipid biomarkers and pollen records from lake sediments. *Geology*, **30**, 463–466.

SEGURA, F., PARDO, J. & SANJAUME, E. 1997. Evolución cuaternaria de la albufera de Torreblanca. *Cuaternario y Geomorfología*, **11**, 3–18.

SERANDREI BARBERO, R. 1975. Il sondaggio venezia 2: stratigrafia e paleoecologica. *Giornale de Geologia*, **XL**, 163–180.

SILLIMAN, J. E., MEYERS, P. A. & BOURBONNIERE, R. A. 1996. Record of postglacial organic matter delivery and burial in sediment of Lake Ontario. *Organic Geochemistry*, **24**, 463–472.

TENZER, G. E., MEYERS, P. A., ROBBINS, J. A., EADIE, B. J., MOREHEAD, N. R. & LANSING, M. B. 1999. Sedimentary organic matter record of recent environmental changes in the St. Marys River ecosystem, Michigan-Ontario border. *Organic Geochemistry*, **30**, 133–146.

TORRES, T., LLAMAS, J. F., CANOIRA, L., COELLO, J., GARCÍA-ALONSO, P. & ORTIZ, J. E. 2000. Aminostratigraphy of two marine sequences from the Mediterranean coast of Spain. Cabo de Huertas (Alicante) and Garrucha (Almería). *In*: GOODFRIEND, G. A., COLLINS, M. J., FOGEL, M. L., MACKO, S. A. & WEMILLER, J. F. (eds) *Perspectives in Amino Acid and Protein Geochemistry*. Oxford University Press, New York, 263–278.

TORRES, T., ORTIZ, J. E., ARRIBAS, I., DELGADO, A., JULIÀ, R. & MARTÍN-RUBÍ, J. A. 2010. Geochemistry of *Persistrombus latus* Gmelin from the Pleistocene Iberian realm. *Lethaia*, **43**, 143–163.

USERA, J., BLÁZQUEZ, A. M., GUILLEM, J. & ALBEROLA, C. 2002. Biochronological and paleoenvironmental interest of foraminifera lived in restricted environments: application to the study of the western Mediterranean Holocene. *Quaternary International*, **93–94**, 139–147.

USERA, J., BLÁZQUEZ, A. M., GUILLEM, J. & ALBEROLA, C. 2006. Evolución holocena de la Marjal de Peñíscola (Castellón, España) deducida del estudio de sus foraminíferos fósiles. *Revista Española de Micropaleontología*, **38**, 381–393.

VIÑALS, M. J. 1995*a*. Secuencias estratigráficas y evolución morfológica del extremo meridional del Golfo de Valencia (Cullera-Dénia). *In*: GRUP VALENCIÀ QUATERNARI (ed.) *El Cuaternario del País Valenciano*. University of Valencia, Valencia, 163–167.

VIÑALS, M. J. 1995*b*. Formaciones litorales fósiles en la costa de Moraira (Alicante). En El Cuaternario del País Valenciano. *In*: GRUP VALENCIÀ QUATERNARI (ed.) *El Cuaternario del País Valenciano*. University of Valencia, Valencia, 187–192.

VIÑALS, M. J. 1996. *El Marjal Pego-Oliva. Evolución geomorfológica*. Consejería de Agricultura y Medio Ambiente de la Generalitat Valenciana, Valencia.

VIÑALS, M. J. & FUMANAL, M. P. 1995. Quaternary development and evolution of the sedimentary environments in the central Mediterranean Spanish coast. *Quaternary International*, **29/30**, 119–128.

VIÑALS, M. J., MATEU, G., FUMANAL, M. P., USERA, J. & FAVERO, V. 1989. Aportación al conocimiento de las facies lagunares y litorales de la Marjal de Oliva-Pego (Valencia). *Cuaternario y Geomorfología*, **3**, 93–104.

VISO, A. C., PESANDO, D., BERNARD, P. & MARTY, J. C. 1993. Lipids components of the Mediterranean seagrass Posidonea Oceanica. *Phytochemistry*, **34**, 381–387.

WEHMILLER, J. 1984. Interlaboratoy comparison of amino acid enantiomeric ratios in fossil molluscs. *Quaternary Research*, **22**, 109–120.

WEHMILLER, J., MILLER, G. *ET AL*. 2010. Interlaboratory comparison of amino acid D/L values. *Geological Society of America Annual Meeting (31 October–3 November 2010), Denver, Colorado, Abstracts with Programs*, **42**, 86.

YLL, E. I., PANTALEÓN-CANO, J. & PÉREZ-OBIOL, R. 1994. Análisis polínico de una secuencia holocénica en Roquetas de Mar (Almería). *In*: MATEU, I., DUPRÉ, M., GÜEMES, J. & BURGAZ, M. E. (eds) *Trabajos de palinología básica y aplicada*. Universidad de Valencia, Valencia, 189–198.

ZAZO, C. 1999. Interglacial sea levels. *Quaternary International*, **55**, 101–113.

ZAZO, C., GOY, J. L. *ET AL*. 2003. Pleistocene raised marine terraces of the Spanish Mediterranean and Atlantic coasts: records of coastal uplift, sea-level highstands and climate changes. *Marine Geology*, **194**, 103–133.